Applied Energy 230 (2018) 374–392

Contents lists available at ScienceDirect

Applied Energy

journal homepage: www.elsevier.com/locate/apenergy

System-level assessment of reliability and resilience provision from microgrids

Yutian Zhou[a], Mathaios Panteli[a], Rodrigo Moreno[b,c], Pierluigi Mancarella[a,d,*]

[a] School of Electrical and Electronic Engineering, The University of Manchester, Manchester M13 9PL, UK
[b] Department of Electrical Engineering, Universidad de Chile, Santiago, Chile
[c] Department of Electrical and Electronic Engineering, Imperial College London, London SW7 2AZ, UK
[d] Department of Electrical and Electronic Engineering, The University of Melbourne, Melbourne, VIC 3010, Australia

HIGHLIGHTS

- Microgrids provision of reliability and resilience is quantified at system-level.
- Multiple sources of uncertainty are modelled using probabilistic capacity tables.
- Long supporting duration differentiates resilience services from reliability ones.
- Probabilistic metrics are defined to indicate microgrids' capacity contribution.
- Aggregation of microgrids at system-level demonstrates significant synergic effect.

ARTICLE INFO

Keywords:
Microgrid
Reliability
Resilience
Energy storage
Distributed energy resources
Power system reserves

ABSTRACT

Microgrids are emerging to coordinate distributed energy resources and locally increase reliability to expected events and resilience to extreme events. Furthermore, by deploying their inherent flexibility, grid-connected microgrids are capable to provide different services at the system-level too. However, these are often assessed independently and a comprehensive integrated framework that can assess benefits for the whole power system is missing. In this outlook, this paper introduces a system-level assessment framework based on the concept of different duration's reserve services that can be provided by microgrids to the main electricity grid in response to both credible (reliability-oriented) and extreme, possibly unforeseen (resilience-oriented) contingencies. Probabilistic capacity tables accounting for different sources of uncertainty related to both microgrids' operation and occurrences of unfavorable events are built to assess the microgrids' potential capacity contribution to a particular reserve service. Case studies based on representative microgrids and a British test system clearly illustrate and quantify how aggregation of microgrids could provide significant contribution to both short-term reliability and longer-duration resilience services far beyond the simple summation of the individual contributions, thus demonstrating a clear synergic effect, as well as the key role played by different forms of energy storage. The proposed framework can assist policy makers and regulators on the strategic role of microgrids for energy system planning and policy developments, including design of ancillary services markets not only to enhance system reliability but also resilience.

1. Introduction

1.1. Background and literature review

Energy systems are undergoing revolutionary changes, which are driven by various reasons including climate change [1], energy efficiency [2], system resilience [3] and the advancement of new technologies [4,5]. One of these changes is the integration of grid-connected microgrids formed by distributed energy resources, such as combined heat and power (CHP), solar photovoltaic (PV), and energy storage (thermal and electrical). New services to exploit flexibilities of grid-connected microgrids for improving the performance of energy systems are hence becoming available to the system operators [5,6]. As it has been pointed out by Mancarella [5,6] and Capuder [7],

* Corresponding author at: School of Electrical and Electronic Engineering, The University of Manchester, Manchester M13 9PL, UK.
E-mail addresses: yutian.zhou@manchester.ac.uk (Y. Zhou), mathaios.panteli@manchester.ac.uk (M. Panteli), rmorenovieyra@ing.uchile.cl, r.moreno@imperial.ac.uk (R. Moreno), p.mancarella@manchester.ac.uk, pierluigi.mancarella@unimelb.edu.au (P. Mancarella).

https://doi.org/10.1016/j.apenergy.2018.08.054
Received 30 April 2018; Received in revised form 2 August 2018; Accepted 11 August 2018
Available online 29 August 2018
0306-2619/

microgrids present more technical and economic value when these distributed multi-energy resources are coordinated at community-level, compared with those values presented on their own. Most importantly, coordinating complementary technologies in microgrids can exploit their flexibility to provide a diverse range of services to the main electricity grid, as suggested by Good [8], Martinez-Cesena [9], Neyestani [10], Mancarella and Chicco [11].

One of the key benefits from grid-connected microgrids is their potential capability to enhance the reliability and resilience of the main electricity grid, in addition to the support to their internal customers during contingencies [12,13]. More specifically, the traditional reliability concept and its principles focus on credible or known contingencies associated with high probability low impact events [3,14]. Particularly, power system security, as a key aspect of reliability, can be effectively maintained by committing operating reserve in order to be prepared for short periods of the system experiencing unexpected increase in demand or generation unavailability within a "credible" range [15]. On the other hand, power system resilience [16] (to which power system engineers are drawing more and more attention) emphasizes the system's response to extreme and rare events, or high impact low probability events [3] and [17–19]. In this context, traditional operating reserve typically with short supporting duration (such as up to 2 h [15]) may not be able to effectively help the system overcome those unfavorable and highly impactful events (e.g., wind storms [3]) requiring a prolonged restoration period, and thus leading to the potential need for new reserve services featuring prolonged supporting duration for resilience enhancement (for instance a period of 24 consecutive hours while the system is being restored, possibly following a black system event). In fact, the literature has demonstrated that microgrids have the potential and capability to contribute to both reliability (in particular security) and resilience. For instance, as investigated by Martinez-cesena [9] and Syrri [20], in addition to the self-sufficient operation as islands, operating reserve services for balancing system demand and a new reliability service for accelerating the restoration of supply to neighboring customers (which can be seen as the reserve for disruptions in distribution network) can be provided by microgrids using their electricity generation capacity surplus (i.e., the microgrid's capacity that is not utilized to supply its internal customers). Besides, Wang [21] and Chen [22] investigated how to dynamically split a distribution network into multiple microgrids in the aftermath of natural disasters, while prioritizing the restoration of critical customers. More recently, it has been highlighted by Li [23] and Chen [24] that the main benefit from grid-connected microgrids lies in their ability to help each other as well as to supply neighboring customers during extreme events. Aki [25] reviewed real-life contribution from microgrids in Japan, where immediate supply to critical customers was provided by PV and batteries but for a relatively short duration and further supply was sustained by gas-fired distributed generators (assuming the presence of an unaffected gas network) until full restoration of the system.

1.2. Relevance, novelty and contribution

Distributed microgrids can be the key means of renewable integration and providers of various services to the legacy energy system for achieving sustainability, reliability and resilience at multiple scales (including community level [26–28] as well as national level [29–31]). In this light, the system-level assessment of multiple services and potential benefits is crucial to inform on the strategic role that microgrids could play, including for system-planning and policy developments [32]. More specifically, this provides insights into the optimal use of energy resources distributed across a sustainable energy system (in particular a sustainable electricity system); and in addition this can also guide energy policy makers, system regulators, industrial stakeholders as well as prospective investors to incentivize, regulate and also invest in the implementation of such microgrids, with a transparent understanding of their potential value presented at the system-level.

However, only few studies [9,20] have laid particular emphasis on their system-level contribution to the main electricity grid during stressed conditions, such as providing various reserve services. Additionally, there have been no studies focusing on the system-level quantification of to what extent microgrids can contribute to both reliability and resilience of the main grid via various reserve services, including both traditional, reliability-oriented operating reserve services (with relatively short service durations) for enhancing system security and resilience-oriented services featuring prolonged duration. This is therefore the research gap that this paper aims to fill.

In fact, for example according to National Grid [33] the total capacity of small-scale (less than 1 MW) CHP units will gradually increase to over 900 MW by 2040; while the total capacity of all distributed CHP units will reach 2,348 MW. These CHP units will have the potential to operate as microgrids, and therefore it becomes critical to quantify to what extent they can contribute to system operation. Similarly, the PV installation, mostly domestic rooftop panels, in the British electricity system is expected to be 36.7 GW by 2040, and when coupled to distributed electricity storage (expected to have an installed capacity of 12.5 GW by 2040 [33]) they could contribute to different services [34].

On the above premises, the objectives of the research work presented in this paper, which are also the main novelties and contributions, are to develop a framework for quantifying the electricity capacity contribution from microgrids to the main electricity grid through various reserve services in different timescales, also including:

- the definition of a probabilistic capacity table for a microgrid as well as the approach for building such probabilistic capacity table with consideration of both operation-related and service-related uncertainties (i.e., those originated by changing operating conditions within the microgrid –including operation of flexible demand, storage and availability of renewables–, and by the occurrence of unfavorable events in the main electricity grid creating the necessity to call upon reserve services);
- the optimization model for evaluating the electricity generation capacity surplus of a microgrid over a particular service in real time (i.e., when reserve services are exercised);
- the consideration of a newly introduced reserve service with prolonged service durations for enhancement to system resilience;
- the approach for aggregating the probabilistic capacity tables of individual microgrids so as to determine the aggregated contribution at system-level, and;
- the metrics for quantifying the electricity capacity contribution from microgrids to reserve services at system-level.

In particular, the proposed assessment framework and modelling approach has to take proper account of the constraints imposed by the operation of microgrids, considering an array of system conditions driven by operation-related and service-related uncertainties that may affect microgrids' capability to provide the indicated reserve services. In this light, similar to the classic *Capacity Outage Probability Table* used in analytical assessments of power system reliability [14], probabilistic capacity tables associating states of certain amount of available capacity surplus with their corresponding likelihoods are applied in the proposed framework so as to take account of those uncertainties.

1.3. Paper structure

The remainder of the paper is organized as follows: Section 2 introduces the general framework for quantifying the electricity capacity contribution from microgrids, including: the definition and creation of the probabilistic capacity table for an individual microgrid, and the optimization model proposed for evaluating the electricity generation

capacity surplus of a microgrid over a particular service in real time[1]; in addition, the adopted model for the scheduled operation of microgrids under planned, normal or expected conditions is also briefly introduced. Section 3 presents the proposed system-level assessment methodology as well as the metrics defined to provide concise quantification. The case study application based on two representative types of microgrids within the context of the British system is demonstrated in Section 4. Finally, Section 5 concludes the paper.

2. Assessment framework and modelling approach for an individual microgrid

This section presents the general framework for quantifying the electricity capacity contribution from a microgrid to reserve services at system-level, when considering both operation-related and service-related uncertainties, as introduced below:

- The operation-related uncertainties include weather conditions, energy market prices and price signals for reserve services. These uncertainties have direct impacts on microgrids' internal energy demand and their scheduled or planned operation with the objective to minimize energy cost and to maximize revenue.
- The service-related uncertainties focus on the starting time of various reserve services and the service duration (thus as mentioned in the Introduction tackling reliability-events of shorter duration as well as resilience-events of longer duration) during real time operation.

With consideration of the above uncertainties, probabilistic capacity tables can be built for individual microgrids to represent their technical capability to deploy their electricity generation capacity surplus (i.e., the microgrid's capacity that is not utilized to supply its internal customers) to supply neighboring customers. The general framework is described in detail as follows.

2.1. General framework for modelling an individual microgrid

The proposed framework can be represented by the flowchart in Fig. 1, which considers the operation-related uncertainties in the outer layer (i.e., those related to scheduled or planned operation) and the service-related uncertainties in the inner layer (i.e., those related to the exercise of the service in real time).

The outer layer firstly considers a database of weather conditions to model the energy demand (including both electricity and heat due to the typical background of multiple energy vectors) and availability of renewable energy resources. This database of weather conditions also represents the corresponding uncertainty set of energy demands and renewable availabilities. More specifically, this database can be created using historical data of weather conditions (such as temperatures and solar irradiance), which inherently captures the uncertainty in weather conditions along with their correlations. On the other hand, it can also be built using weather simulation software, which generates weather conditions based on statistical features (thus the uncertainty) of weather conditions (such as the Weather Generator tool developed under the UK Climate Change Projections [35]). Afterwards, this database is taken as input to the high resolution simulator for multi-energy domestic demand profiles, as developed in [36] (where a diversity of appliances and occupancy profiles are further considered). Meanwhile, solar irradiance and temperatures in the database are used to calculate the power outputs of PV panels [37]. Additionally, it is worth noting that this database outlined in the framework is flexible (meaning it can be built via different means as mentioned earlier) to accommodate further uncertainties or scenarios if desired.

The scheduled or planned operation model of microgrids is another key part of the outer layer in Fig. 1. This planned operation model determines the operating statuses of the energy resources in a microgrid, particularly the state of charge (SOC) of energy storage (which is critical for exploiting microgrids' flexibility). For instance, the CHP unit in a microgrid can use its spare electricity generation on condition that the accompanying heat production can be consumed internally or stored in thermal energy storage; similarly, a microgrid with PV panels may rely on batteries to maintain a stable contribution of electricity capacity, or its batteries may be the sole source of electricity capacity. In this light, the SOC of energy storage (electrical or thermal) at the starting time of delivering a specific reserve service is key to assess the contribution from microgrids to security and resilience. In other words, this is the energy-limited feature of microgrids. Eventually, the planned operation model of microgrids provides the profiles indicating chronological operating statuses of these energy storage units.

The inner layer in Fig. 1 captures the service-related uncertainties (i.e., the starting time and service duration) during real time. Microgrids may provide reserve services to the main electricity grid at any time, leading to various service starting times. Additionally, the service duration is another key factor in the proposed optimization model. As mentioned earlier, traditional operating reserve typically requires a service duration of about two hours [15]. On the other hand, this paper also lays emphasis on reserve services with prolonged service durations (e.g., 24 h), aiming to enhance the system resilience to rare events with extreme (and in this case prolonged) impacts. In this light, the inner layer assesses the microgrid's electricity generation capacity surplus considering various starting times and durations of reserve services. Thus, a database of the electricity capacity contributed by microgrids can be obtained in the end. This database can hence be used to build probabilistic capacity tables subject to specific service durations.

As a further remark, the benefit (i.e., the electricity capacity contribution) from microgrids lies in their capability to supply the electricity demand in their vicinities. More specifically, the System Operator would see short periods of reduction in the system demand when the reserve for security provided by microgrids is exercised. On the other hand, the new reserve service for resilience would be seen as microgrids supplying neighboring customers for a prolonged period of time until the restoration of the system. Nonetheless, networks connecting the microgrids to their vicinity are not explicitly modelled in this framework. This is because the microgrids affected by disrupted networks cannot contribute unless these networks are restored. This impact of networks is not relevant to the internal characteristics and operation of microgrids.

Furthermore, it is also acknowledged that the system-level contribution from microgrids comes from and heavily relies on the cooperation and other interactions of these microgrids. As highlighted in [38] and [39], the cooperation of microgrids is crucial to maximizing the utilization of these distributed energy resources within the microgrids. In this line, in order to quantify the maximum capacity contribution from microgrids as well as allow transparent implications to be drawn at the system-level, (prefect) cooperation is assumed to be achieved by cost-minimising operation of the aggregated microgrids when providing reserve services to the main electricity grid. Further studies in cooperation issues, albeit very important, are beyond the scope of this paper and are suggested as future work.

2.2. Evaluation of capacity contribution from an individual microgrid to various reserve services

This section presents the definition of the electricity capacity contribution from a microgrid to various reserve services that, as

[1] In this paper, *real-time* operation refers to the operation during the utilization or exercise of a reserve service during its delivery in real time so as to support the main electricity grid under a contingent event, while *planned or scheduled* operation refers to the operation determined ahead of real time, when idle capacity margins can be booked.

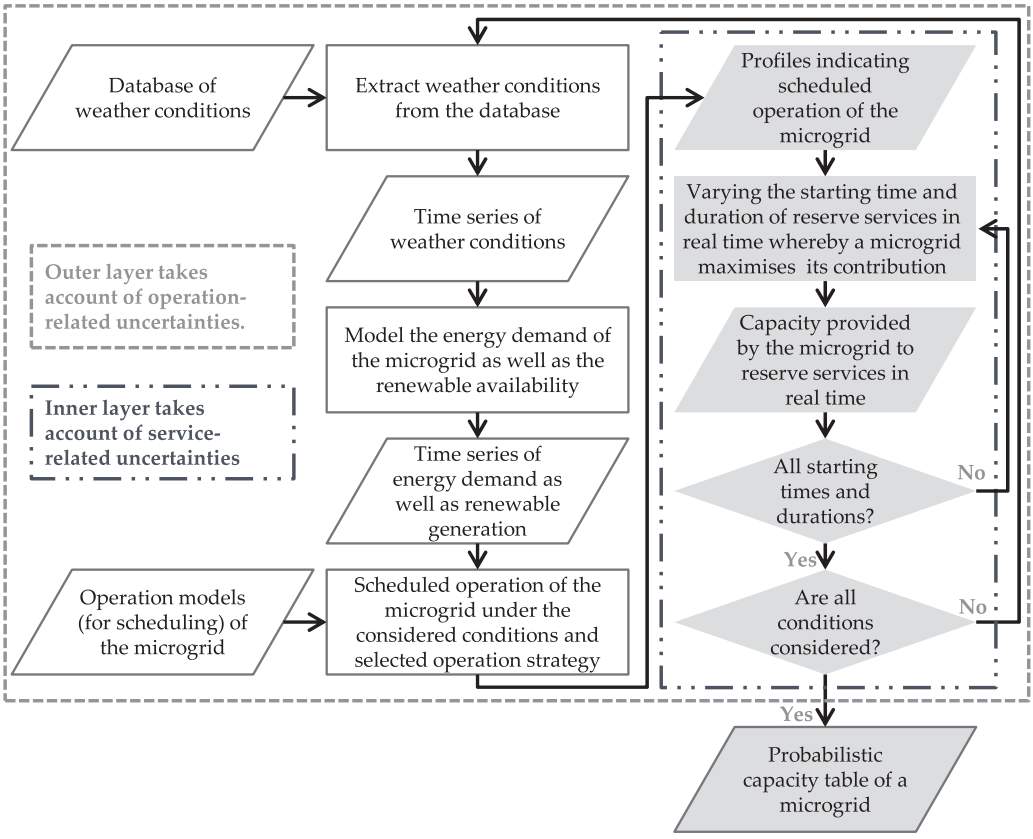

Fig. 1. General framework for evaluating the electricity capacity contribution from microgrids.

highlighted in the Introduction, are differentiated by the service duration (particularly in this paper we consider a range of service durations from 1 to 24 h). These services are used to provide support to the main electricity grid in case unfavorable conditions occur and thus they can be exercised at any time by the System Operator. This section also presents the optimization-based assessment model for evaluating that contribution by maximizing the utilization of microgrid's electricity generation capacity surplus in real time (particularly when the microgrid is oversized for economic benefits [40,41]). Importantly, note that this optimization problem is related to the real time operation of the microgrid (as explained in this Section 2.2), while the planned operation (determined before this contribution is evaluated) is obtained by another optimization problem as explained in Section 2.3.

2.2.1. Definition of the electricity capacity contribution to reserve services

The System or Network Operator would have certain requirements on reserve provision (such as those required by the British system operator [15]), i.e., a consistent amount of electricity capacity provided, which if called upon in real time, has to be maintained during a specific time window. Importantly, in the absence of energy storage, it is clear that the capacity surplus at a given time will be simply the difference between the available generation capacity minus demand within the microgrid and this can be assessed by using the planned or scheduled operating condition. However, the presence of energy storage within the microgrid originates the need to test the effects of exercising reserve services in real time, assessing how much and for how long a given export level (i.e., the difference between generation output and internal demand in real time) can be maintained from the microgrid to the rest of the system (this will be mathematically introduced later on in Section 2.2.3).

For instance, Fig. 2 demonstrates the available generation capacity, the planned and real time generation dispatches and the evolving generation capacity surplus of a microgrid during a typical summer weekday in England. This microgrid has a gas-fired CHP unit with an electricity generation capacity of 51 kW, as modelled in [9]. Further, Fig. 2 illustrates a constant available generation capacity due to the nature of the generation technology (i.e., CHP); on the contrary, in the case a microgrid features variable renewable generation (e.g. PV), the available generation capacity would be changing over time. Planned and real time generation dispatches are differentiated when reserve services are utilized, increasing generation outputs in real time to support the main electricity grid in case a contingent event happens.

In Fig. 2, the capacity surplus (i.e., the difference between the available generation capacity P_{avail} minus the planned generation dispatch $P_{planned}$) is changing over the entire 24-h horizon. Particularly, the capacity surplus is utilized from t_0 to t_1 to support the main system; note that the minimum contribution is denoted as C_1 (assuming the real time generation $P_{real-time}$ output is equal to P_{avail}). Therefore, when we refer to the capacity contribution associated with a reserve service from a microgrid, we use the term *minimum capacity surplus* since capacity surplus can vary across a time window (for example, due to a change in internal demand) and we use the minimum value within that window as the capacity that a microgrid can really commit for the security of the main electricity system (later on in Section 2.2.3 we show that this minimum value is maximized in real time operation of the microgrid).

Further, as highlighted earlier, the service duration is considered in this paper to differentiate the reserve services for reliability (or more accurately security) from those for resilience. In this light, a threshold can be specified for reserve services to define security-related services and resilience-related services, i.e., a service with a duration less than the threshold is classified as a security service, while one with a duration greater than the threshold is classified as a resilience service.

It has to be noted that this threshold for service duration is highly system-specific. For instance, in the context of the British system, the

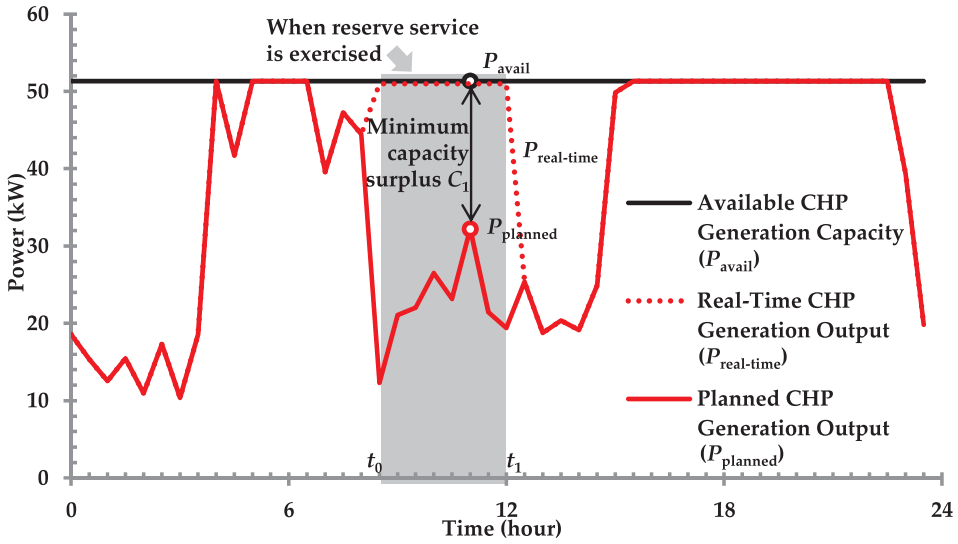

Fig. 2. Demonstration of electricity capacity contribution from a microgrid.

cold start time (from notice to full load) of a combined cycle gas turbine[2] (CCGT) is typically from 3.5 to 4 h [42], while it is expected to take a crew 5 h to restore supply to the affected customers in a distribution network [9]. This means that under stress conditions the system "normally" needs support within the first 5 h. Therefore, in this paper the threshold for the service duration is specified to be 5 h, i.e., a reserve service lasting equal to or less than 5 h is considered to be security-related services, whereas a reserve service lasting more than 5 h is categorized as resilience-related services. Note that this threshold can be changed to another similar value without affecting our main observations and conclusions.

2.2.2. Probabilistic capacity table for a microgrid

With consideration of the aforementioned uncertainties, a set of minimum electricity generation capacity surpluses can be calculated through the simulation of various scenarios (see Fig. 2), which can be further used to build a probabilistic capacity table for a microgrid.

The probabilistic capacity table is defined as a discrete probability distribution over the range between zero and N_C (i.e., the table length corresponding to the maximum available capacity) with steps of one capacity interval ΔC (which is specified depending on the requirement on accuracy, i.e., the smaller the capacity interval ΔC the higher the accuracy, as the more capacity states the table can represent). Each capacity state i (which varies from zero to N_C) represents an available capacity equal to i multiplied by ΔC and the capacity state i is associated with a probability $p(i)$ corresponding to the likelihood of having the available capacity of i multiplied by ΔC. For instance, assuming a microgrid can present a maximum generation capacity surplus of 100 kW and the capacity interval ΔC is 20 kW, a probabilistic capacity table in Table 1 can be built for the microgrid (note that, for this example, the probabilities are arbitrary).

Let K be the set of minimum electricity generation surpluses $C_{\min,k}$ that are determined for the reserve services (varying starting times but the same duration), and N_K be the size of the set. Then, the table length N_C can be calculated from (1). Afterwards, the probability of a capacity state $p(i)$ can be calculated from (2) using indicator functions $\mathbf{I}_i(C_{\min,k})$, which are defined in (3) when i is 0; and in (4) when i is greater than 0.

$$N_C = \text{Round}(\text{Max}\{C_{\min,k} \in \mathbf{K}\}/\Delta C) \tag{1}$$

[2] In the British system, CCGT as key intermediate generation plays an essential role in maintaining the system's secure operation due to its operational flexibilities (such as the start-up time and ramping up rate) [31].

Table 1
Demonstration of a probabilistic capacity table.

Capacity state $\boldsymbol{i}$	0	1	2	3	4	5
Probability $\boldsymbol{p(i)}$	0.1	0.2	0.4	0.15	0.1	0.05
Available capacity $i{\cdot}\Delta C$ (kW)	0	20	40	60	80	100

$$p(i) = \sum_k \mathbf{I}_i(C_{\min,k})/N_{\mathbf{K}},\ C_{\min,k} \in \mathbf{K} \tag{2}$$

$$\mathbf{I}_0(C_{\min,k}) = \begin{cases} 1, & C_{\min,k} \in [0,\ 0.5{\cdot}\Delta C] \\ 0, & \text{otherwise} \end{cases} \tag{3}$$

$$\mathbf{I}_{i>0}(C_{\min,k}) = \begin{cases} 1, & C_{\min,k} \in [(i{-}0.5){\cdot}\Delta C,\ (i+0.5){\cdot}\Delta C] \\ 0, & \text{otherwise} \end{cases} \tag{4}$$

According to the calculation in (2)-(4), the capacity interval ΔC can affect the probability of a capacity state $p(i)$, leading to an impact on the assessment accuracy. Thus, for individual microgrids a small capacity interval is more accurate, as it can capture more capacity states. On the other hand, when the total contribution of a number of microgrids is assessed and aggregated at system-level, it may become necessary to increase the capacity interval while aggregating the probabilistic capacity tables. In this light, the calculation in (5) and (6) is proposed to increase the capacity interval. Let $\Delta C'$ be the new capacity interval and N_C' be the new table length, which can also be calculated based on (1) using $\Delta C'$.

$$p'(j) = 0, \text{ for all} j = 0,\ 1,\ 2,\ \ldots, N_C' \tag{5}$$

$$p'(j) = p'(j) + p(i),\ j = \text{Round}\left(i{\cdot}\frac{\Delta C}{\Delta C'}\right),\ \text{for all} i = 0,\ 1,\ 2,\ \ldots, N_C \tag{6}$$

2.2.3. Real time optimization for evaluating electricity capacity contribution to reserve services

The optimization model is proposed to determine real time operation by maximizing the minimum electricity generation capacity surplus of a microgrid in a specific scenario where the reserve service is exercised. This is different to the scheduled or planned microgrids' operation where some capacity room might be booked but not actually utilized, as the model shown later in Section 2.3. By focusing on the technical constraints imposed by internal energy demand, renewable energy resources and storage, a microgrid is assumed to operate for reserve provision with the objective to maximize its minimum

electricity generation capacity surplus (i.e., the minimum surplus is the level that can be committed to support the main electricity grid, see Fig. 2) subject to its internal energy and reliability constraints. The maximization problem is justified since we want to determine the potential, maximum security or resilience support from a microgrid to the main electricity grid. In this context, the following formulation is proposed.

Additionally, the presented optimization assumes perfect forecasting for energy demand and renewable availability. This may not be ideal in terms of performing short-term operation scheduling for individual microgrids (although we do acknowledge the presence of uncertainty –in a deterministic way- by scheduling reserve capacities). Nonetheless, using typical days to represent the uncertainty and variation of energy demand and renewable generation is generally applied in academic research [2,7,8], long-term planning methods and tools employed by relevant industries in the UK [43], as well as technical consulting reports for resource planning published on behalf of governments [44]. Similarly, as the aim of the paper is to inform on the strategic role that microgrids could play in long-term system-planning and policy developments, it would be adequate to represent the uncertainty and variation of energy demands and renewable generation in microgrids particularly with consideration of various typical days of weather conditions in the outer layer of the assessment framework in Fig. 1.

- Objective function

The objective function maximizes the minimum electricity generation capacity surplus during a service window. Let W be the number of time steps included in a service window and t represents a time step. The electricity generation capacity surplus is denoted by C, where the subscript "min" is for minimum.

$$\text{Maximize:} C_{\min} \tag{7}$$

$$\{C_{\min} \geqslant C_t,\ t = 1,\ 2,\ \ldots, W\} \tag{8}$$

The evolving electricity generation capacity surplus C_t can be calculated from (9). P refers to the real time dispatch with consideration of CHP units, PV panels and batteries (for the sake of clearness and without loss of generality), which are denoted by the subscripts "CHP", "PV", "Chg" and "Disc" (corresponding to *charging* and *discharging*), respectively. The subscript "D" in (9) represents the total internal electricity demand of that microgrid. It has to be noted that C_t can be also understood as the "exporting" power from a microgrid and it might be also a negative value (a deficit of internal supply leading to the need for a power import), due to the intermittency of renewable generation, changing demand and the energy-limited nature of energy storage. It has to be noted that other distributed resources can also be included as appropriate.

$$C_t = P_{\text{CHP},t} + P_{\text{PV},t} + P_{\text{Disc},t} - P_{\text{Chg},t} - P_{D,t} \tag{9}$$

- Model of CHP unit

A CHP unit generates electricity and heat at the same time. In order to use its spare electricity generation, the accompanying heat production has to be consumed or stored in thermal energy storage. Let H be the heat production and it can be calculated from (10), where η^e and η^h represent the electricity and heat efficiencies, respectively. Additionally, the maximum electricity capacity of the CHP unit is constrained in (11).

$$H_{\text{CHP},t} = P_{\text{CHP},t} \cdot \frac{\eta^h}{\eta^e} \tag{10}$$

$$P_{\text{CHP},t} \leqslant P_{\text{CHP,max}} \tag{11}$$

- Model of thermal energy storage

Thermal energy storage is modelled in order to provide CHP units the flexibility of continuing to generate electricity when the accompanying heat production becomes excessive. The SOC of thermal energy storage at the next time step ($S_{\text{Heat},t+1}$) can be calculated from (12) based on the SOC at the current time step ($S_{\text{Heat},t}$), the CHP heat production ($H_{\text{CHP},t}$), the thermal loss ($H_{\text{Loss},t}$) and the heat demand ($H_{\text{Dem},t}$). Additionally, an alternative heat supply source ($H_{\text{Alt},t}$) is assumed when the CHP is sized based on the electricity peak demand of the microgrid, rather than the heat peak demand. For instance, this alternative heat supply source can be gas boilers, as in the case study application later. According to [9], the thermal loss can be calculated from (13), where Y_{Therm} and R_{Therm} represent the thermal capacitance and the thermal resistance of thermal energy storage; in addition, the length of a time step is denoted by Δt and the ambient temperature surrounding the thermal energy storage is denoted by T_t. Moreover, the size of thermal energy storage can be represented by the maximum and minimum temperatures, which are denoted by $T_{\max}$ and $T_{\min}$ as in (14). Furthermore, the SOC of thermal energy storage at the beginning of a service window ($S_{\text{Heat},0}$) relies on the planned operation of the microgrid, which is an input from the outer layer depicted in Fig. 1.

$$S_{\text{Heat},t+1} = S_{\text{Heat},t} + (H_{\text{CHP},t} - H_{\text{Dem},t} - H_{\text{Loss},t} + H_{\text{Alt},t}) \cdot \Delta t \tag{12}$$

$$H_{\text{Loss},t} = \frac{\frac{S_{\text{Heat},t}}{Y_{\text{Therm}}} - T_t}{R_{\text{Therm}}} \tag{13}$$

$$(T_{\min} - T_t) \cdot Y_{\text{Therm}} \leqslant S_{\text{Heat},t} \leqslant (T_{\max} - T_t) \cdot Y_{\text{Therm}} \tag{14}$$

- Model of electrical energy storage

Electrical energy storage (e.g., batteries) provides flexibility for microgrids particularly in the presence of distributed renewable generation. More specifically, the SOC of electrical energy storage at the next time step ($S_{\text{Elec},t+1}$) can be calculated from (15) taking account of the SOC at the current time step ($S_{\text{Elec},t}$) as well as the charging ($P_{\text{Chg},t}$) and discharging ($P_{\text{Disc},t}$) powers of batteries. The charging and discharging efficiencies are denoted by $\delta^+$and δ^- in (15); in addition, binary variable b_t is used to indicate whether the batteries are charging (i.e., $b_t = 1$) or discharging (i.e., $b_t = 0$).

Constraints in (16) and (17) would make sure that the energy and power limits of batteries are respected and batteries can only be charged by local distributed generators in service operation (e.g., PV panels in (18)). The constraint in (19) represents the requirement on the SOC of batteries ($S_{\text{Elec,req}}$) at the end of a service window. Similarly, the SOC of electrical energy storage at the beginning of a capacity service window ($S_{\text{Elec},0}$) also depends on the planned operation of the microgrid, which is an input from the outer layer depicted in Fig. 1.

$$S_{\text{Elec},t+1} = S_{\text{Elec},t} + P_{\text{Chg},t} \cdot (1 - \delta^+) \cdot \Delta t - P_{\text{Disc},t} \cdot (1 + \delta^-) \cdot \Delta t \tag{15}$$

$$S_{\text{Elec,min}} \leqslant S_{\text{Elec},t} \leqslant S_{\text{Elec,max}} \tag{16}$$

$$0 \leqslant P_{\text{Chg},t} \leqslant P_{\text{Chg,max}} \cdot b_t,\ 0 \leqslant P_{\text{Disc},t} \leqslant P_{\text{Disc,max}} \cdot (1 - b_t) \tag{17}$$

$$P_{\text{Chg},t} \leqslant P_{\text{PV},t} \tag{18}$$

$$S_{\text{Elec},W} \geqslant S_{\text{Elec,req}} \tag{19}$$

In summary, the optimization problem expressed in (7) and (8) is complemented with the extra constraints in (9)-(19). The optimization will be carried out for each type of reserve service. Reserve services are differentiated by their durations (i.e. timespan in which a given capacity surplus level can be ensured –or *guaranteed* with a given confidence level as explained later on in Section 3.2.1– and delivered from a microgrid to the main electricity grid) and they can be exercised at any time across a day by the System Operator.

2.3. Sheduled operation strategies for individual microgrids

In this work, the proposed framework (as seen in Fig. 1) is not limited to a specific scheduled operation strategy of microgrids. Instead, various scheduled operation strategies can be integrated in the framework and more importantly different scheduled operation strategies will lead to different probabilistic capacity tables of microgrids. This is due to the fact that different scheduled operation strategies might present significantly different impact on the SOC of energy storage. Moreover, this paper focuses on introducing the framework in Fig. 1, rather than developing an optimization for microgrids' planned, normal operation. That being said, the mixed-integer linear programming (MILP) model proposed in [9] for optimizing the operation of microgrids is adopted in this paper.

As modelled in [9], the objective function of a microgrid's scheduled operation is the minimization of the cost of meeting its internal energy demand by purchasing and selling electricity at importing and exporting prices in the electricity market as well as buying gas from the gas market; in addition to trading energy, the objective function can also include a further reduction in the cost (i.e., increase in revenue) by providing reserve services to the main electricity grid at certain price (which is £ 0.00451 per kW per hour as modelled in [9] following the British market information [15]). The aforementioned objective function of microgrids' scheduled operation is optimized subject to the technical constraints of CHP units, gas boilers, PV generation availability, thermal storage and batteries. The scheduled operation strategies introduced here may book certain capacity headroom for reserve services depending on the economic revenue based on the reserve price, rather than exercising the services. As results, profiles of the chronological SOCs of energy storage units are obtained and further utilized to evaluate the actual electricity capacity contribution when reserve services are exercised, as modelled in Section 2.2.3.

Though multiple strategies for scheduled operation were investigated for their economic benefits in [9], this paper, with its objective to quantify microgrids' contribution to the aforementioned reserve services, focuses on the following two strategies for microgrids' scheduled operation based on the optimization model developed in [9].

- Base Strategy: Minimization of Energy Cost

With regard to the Base Strategy, the scheduled operation of microgrids has the sole objective of minimizing their energy cost by purchasing and selling electricity at fixed importing and exporting prices as well as buying gas from gas market. In other words, microgrids only participate in energy arbitrage. This is to demonstrate to what extent microgrids can provide reserve services, though there are no proper incentives from the main electricity grid.

- "Res" Strategy: Minimization of Energy Cost plus Maximization of Revenue via Provision of Reserve Services

With regard to the Res (which stands for "reserve") Strategy, in addition to the minimization of microgrids' energy cost, microgrids' operation is also planned or scheduled to also receive payment for providing reserve services to the main electricity grid. This is for the purposes of quantifying the improvement in the amount of reserve that can be provided by the incentivized microgrids, compared with those microgrids without incentives under the Base Strategy. Thus, if prices of reserve services are sufficiently attractive to be provided by a microgrid, its scheduled operation will feature idle capacity margins that can be, later on, used in real time to export power and provide reserve services to the main electricity grid (this real time operation is determined through the optimization model explained in Section 2.2.3).

3. System-level assessment methodology for aggregated microgrids

This section presents the methodology for assessing the contribution of electricity capacity from aggregated microgrids at system-level. The underlying assumption is that the infrastructure and networks inside the microgrids, as well as the connections between microgrids and upstream grids are intact; so that the microgrids can successfully supply the electricity demand in their vicinity. Further, the probabilistic capacity table of a microgrid is created with specific service durations. This means the following assessment is separately performed for different service durations. More importantly, this allows clear quantification of microgrids' contribution to traditional reserve services with short durations (i.e., for security purposes), as well as new reserve services with prolonged service durations for overcoming extreme events (i.e., for resilience purposes), respectively. Additionally, the microgrids distributed across the main electricity grid are assumed to operate with full cooperation when providing reserve services. From a theoretical point of view, this enables transparent implications at the system-level, focusing on the fundamental trends associated with the availability of resources from microgrids. From a more practical perspective, this serves as an upper bound, determining the maximum amount of capacity support from the microgrids.

3.1. Probabilistic aggregation of electricity capacity contribution from microgrids to reserve services

Electricity capacity contribution from individual microgrids to reserve services with a particular service duration (that is obtained by the process described in Section 2.2.3) is aggregated via convolution of their probabilistic capacity tables, i.e., the discrete probability distribution of the total capacity contribution from these microgrids is the convolution of their individual distributions. The convolution of these probabilistic capacity tables assumes that the operation of these microgrids is independent from each other. It is acknowledged that the closer geographically the more correlated the microgrids are, while assuming independency among microgrids might lead to overestimate their aggregated contribution. On the other hand, the quantification of to what extent dependency among microgrids (such as dependency of resource availabilities and dependency due to responses to the system price signals) can affect their contribution at the system-level to reserve services is therefore suggested as a key future work.

The calculation in (20)-(22) corresponds to the convolution of two probabilistic capacity tables with the same capacity interval. Let $p(i)$ and $p(j)$ represent the two probabilistic capacity tables, while $p(h)$ is the result of this probabilistic aggregation. The table length of $p(h)$ is calculated from (22), where N_{Ci} and N_{Cj} are the table lengths of $p(i)$ and $p(j)$, respectively. Prior to (21), $p(h)$ needs an initialization as in (20).

$$p(h) = 0, \text{ for all} h = 0, 1, 2, \ldots, N_{Ch} \tag{20}$$

$$p(h) = p(h) + p(i)\cdot p(j),\ h = i + j, \text{ for all} i = 0, 1, 2, \ldots, N_{Ci} \text{and all} j = 0, 1, 2, \ldots, N_{Cj} \tag{21}$$

$$N_{Ch} = N_{Ci} + N_{Cj} + 1 \tag{22}$$

3.2. Electricity capacity contribution metrics based on guranteed capacity

This section introduces the metrics defined to indicate the level of capacity contribution from microgrids. The proposed metrics are based on the concept of *guaranteed capacity*, which has been applied to evaluate the capacity value of renewable generation in [45]. The concept of guaranteed capacity is in line with the probabilistic capacity table, and can provide concise quantification of the level of contribution from microgrids, which can be compared with other generation resources on a level playing field.

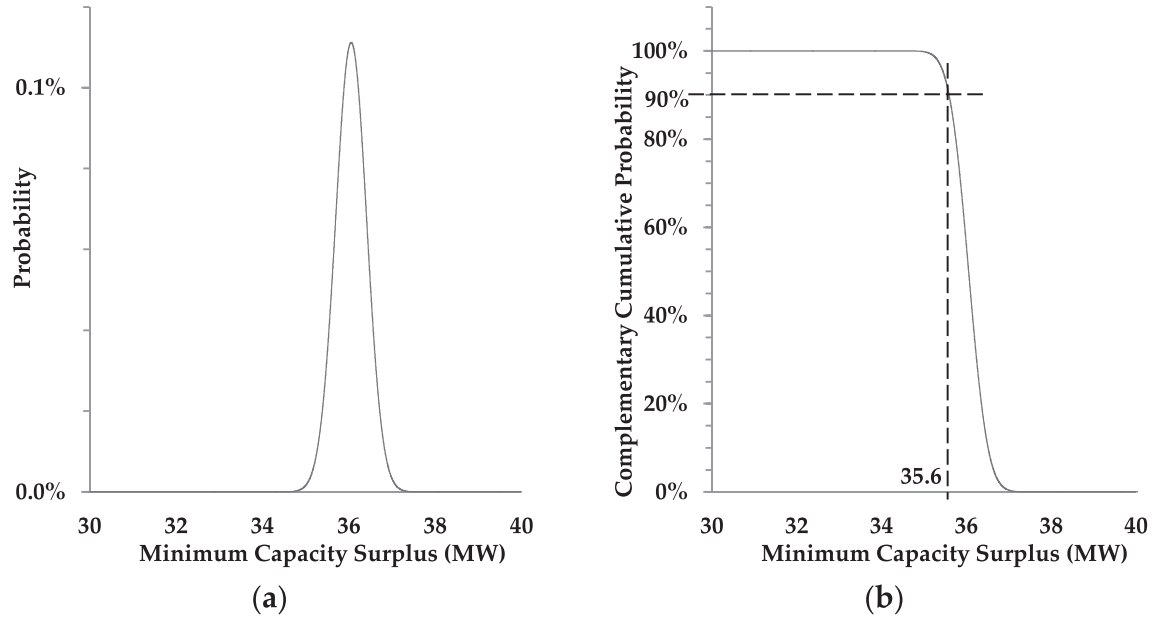

Fig. 3. Available capacity duration curve of 1000 microgrids with a total CHP capacity of 51.4 MW and the guaranteed capacity is of 35.6 MW with a probability of 90%.

3.2.1. Quantification of the guaranteed capacity of microgrids at System-level

As described in [45], the "Guaranteed Capacity" of an electricity supply resource is defined to be the least available electricity capacity that can be expected with a specified probability. In this paper, this metric is adopted to indicate the electricity capacity that microgrids can contribute to reserve services at system-level, based on the aggregated probabilistic capacity table. The evaluation of guaranteed capacity is introduced in detail as follows.

In mathematical terms, the probabilistic capacity table of a number of microgrids (i.e., $p(i)$, $i = 0, 1, 2, ..., N_C$) describes a discrete probability distribution, which can be used to create a complementary cumulative probability distribution as expressed in (23). In the context of this paper, this complementary cumulative probability distribution can be more aptly referred to as an "available capacity duration curve" [45]. Afterwards, with consideration of a specific probability p, the guaranteed capacity of these microgrids can be calculated from (24), where "inf" refers to infimum or the greatest lower bound. An example for evaluating the guaranteed capacity of 1,000 microgrids is shown in Fig. 3.

$$\overline{F}(i) = \sum_{j \geqslant i} p(j), \text{ for all} i = 0, 1, 2, ..., N_C \tag{23}$$

$$C(p) = \Delta C \cdot \inf\{i \in \{0, 1, 2..., N_C\}: \overline{F}(i) \geqslant p\} \tag{24}$$

Fig. 3-(a) presents the probabilistic capacity table $p(i)$ built for these microgrids with a total CHP capacity of 51.4 MW. Afterwards, the available capacity duration curve $\overline{F}(i)$ can be created based on $p(i)$, as seen in Fig. 3-(b). Further, it can be seen in Fig. 3-(b) that with a probability of 90% the guaranteed capacity of these 1000 microgrids is 35.6 MW. The underlying service duration is one hour.

Ultimately, this metric provides a direct value with a specific level of confidence (i.e., the amount of available capacity associated with the corresponding probability) to indicate the level of electricity capacity contribution. Consideration of a confidence level is key; note that, in practice, not even a bulk, grid-connected peaking (very fast and reliable) generating unit can ensure provision of its total idle capacity as a reserve service with a 100% confidence (and this contradicts actual deterministic market design of ancillary services [46]). Therefore, it is important to define a *reasonable* confidence level against which reserve services are guaranteed so as to allow a fair comparison among various resources (from the generation and demand side) for the provision of the services.

3.2.2. Quantification of the additional available capacity of microgrids at System-level

In order to properly evaluate the additional electricity capacity that is made available by these microgrids to the system, the "additional available capacity" metric is defined based on the concept of aforementioned guaranteed capacity.

Firstly, the probabilistic capacity table of the generation system is built through convolution of probabilistic capacity tables of single conventional generators and renewable generation. In order to do so, the probabilistic capacity table of a single conventional generator can be built as in (25) and (26), where a is the average availability of that conventional generator, N_C corresponds to the table length, C_{gen} is the nameplate capacity and $\Delta C_{\text{gen}}$is the capacity interval. It has to be noted that ΔC_{gen} is the capacity interval defined for the generation system, which in general would be much greater than the capacity interval $\Delta C_{\text{mic}}$for individual microgrids.

$$p(i) = \begin{cases} 1-a, & i = 0 \\ a, & i = N_C \\ 0, & \text{otherwise} \end{cases} \tag{25}$$

$$N_C = \text{Round}\left(\frac{C_{\text{gen}}}{\Delta C_{\text{gen}}}\right) \tag{26}$$

Then, similar to microgrids, the probabilistic capacity table of a renewable generation resource can be built as presented from (27) to (30), where G_{ren} is the power output from historical database $\mathbf{R}$ of the renewable generation resource and $N_{\mathbf{R}}$ is the length of the probabilistic table.

$$N_R = \text{Round}(\text{Max}\{G_{\text{ren}} \in \mathbf{R}\}/\Delta C_{\text{gen}}) \tag{27}$$

$$p(i) = \sum_k \mathbf{I}_i(G_{\text{ren}})/N_{\mathbf{R}},\ G_{\text{ren}} \in \mathbf{R} \tag{28}$$

$$\mathbf{I}_0(G_{\text{ren}}) = \begin{cases} 1, & G_{\text{ren}} \in [0,\ 0.5 \cdot \Delta C_{\text{gen}}] \\ 0, & \text{otherwise} \end{cases} \tag{29}$$

$$\mathbf{I}_{i>0}(G_{ren}) = \begin{cases} 1, & G_{ren} \in [(i-0.5)\cdot\Delta C_{gen},\ (i+0.5)\cdot\Delta C_{gen}] \\ 0, & otherwise \end{cases} \quad (30)$$

Further, the probabilistic capacity table of the generation system is obtained via convolution of the above probabilistic capacity tables of conventional generators and renewable generation, which is referred to as $p_{gen}(i)$. Afterwards, the capacity interval ΔC_{mic} of the probabilistic capacity table of a number of microgrids is increased to the capacity interval ΔC_{gen}, as described in (5) and (6); such that, a new probabilistic capacity table of the whole supply resources (both the generation system of the main grid and microgrids) can be computed via convolution of the probabilistic capacity table of the generation system and the one of the microgrids, which is referred to as $p_{all}(i)$.

Moreover, the corresponding availability capacity duration curves $\overline{F_{gen}}(i)$ and $\overline{F_{all}}(i)$ can be obtained based on $p_{gen}(i)$ and $p_{all}(i)$, respectively. According to the definition of guaranteed capacity, with a specified probability p, two guaranteed capacities can be obtained from $\overline{F_{gen}}(i)$ and $\overline{F_{all}}(i)$, which are referred to as $C_{gen}(p)$and $C_{all}(p)$, respectively. Eventually, the difference between $C_{gen}(p)$ and $C_{all}(p)$ is defined as the additional available capacity $A_{MGs}(p)$. Note that this additional available capacity is subject to a particular duration of the reserve service. Fig. 4 illustrates a conceptual example of the evaluation of the additional available capacity of the microgrids.

Unlike the metric "Guaranteed Capacity" introduced earlier that quantifies the level of electricity capacity contribution from the microgrids' point of view, this metric, "additional available capacity", clearly indicates the amount of capacity that is made available (also with a specific confidence/probability) from the perspective of the generation system. In other words, it draws a complete picture for all the supply sources including both the main generation system and microgrids.

4. Case study application

This section demonstrates the case study application using typical types of microgrids based on the models of general British households [36] as well as a test British electricity system for assessing the electricity capacity contribution from microgrids to the system.

4.1. Description of test microgrids and test British electricity system

4.1.1. Test microgrids: energy demand and technology sizing

Two typical types of microgrids are modelled in the case study application. On the one hand, both of the microgrids consist of the same 100 households, which are assumed to be semi-detached houses taking account of a diverse range of appliances and occupancy profiles with consideration of the UK statistics. As modelled in [9], the annual heat and electricity demands, that feature a 30-min resolution, are 826 MWh and 124 MWh, respectively, which have been validated in the studies carried out in [36,47]. Weather data of seven typical days are considered in modelling the energy demand, as shown in Fig. 5, including weekdays (w/d) and weekends (w/e) of winter, summer, shoulder (i.e., spring and autumn) seasons, and a peak day representing the highest demand days (this corresponds to a practice exercised by the British System Operator [48]). The aforementioned seven typical days are therefore used to represent the uncertainty set of energy demands and renewable availabilities in the case study application. In addition, detailed profiles of energy demands, temperatures and PV outputs are provided in Appendix A.

On the other hand, the two typical types of microgrids have distinct energy supply resources. The first test microgrid (referred to as MG1) has a gas-fired CHP unit, a gas boiler and a thermal energy storage, while the second one (referred to as MG2) is equipped with rooftop PV panels and batteries as well as a gas boiler (but no thermal energy storage). Electricity and heat demands are supplied through distribution feeders and a district heating network inside the microgrids.

Table 2 shows the sizing of different technologies. As seen in the table, the CHP unit in MG1 is sized to cover its electricity peak demand (51.4 kWe, see Fig. 5.b), while the rest of the heat peak demand is supplied by the gas boiler. The thermal energy storage is sized to be 210 kWh_{th}, which corresponds to a volume of 7250 L with maximum and minimum temperatures of 80 °C and 55 °C, respectively (determined in [41] using a detailed cost-benefit analysis). The total PV installation in MG2 is 275 kW_p, as suggested by the UK's Energy Savings Trust [49]; meanwhile, the batteries in MG2 is sized at 109.8 kWh for total energy capacity, which is equal to the highest electricity demand for five continuous hours [9], and the total power capacity is 65.9 kW considering 60% for the ratio of power capacity over energy capacity [50].

In summary, MG1 and MG2 represent two distinct types of microgrids. The electricity capacity contribution from MG1 comes from the CHP unit, which can be controlled. Meanwhile, flexibility of MG1 relies on thermal energy storage, which stores the unconsumed heat production accompanying the electricity generation. Unlike MG1, the electricity supply source of MG2 is PV panels, which are intermittent and can be controlled to a limited extent (i.e., generation curtailment). Thus, MG2's key source of flexibility comes from batteries. It has to be highlighted that the two microgrids specifically simulated in this paper are considered to be two distinct and representative types of

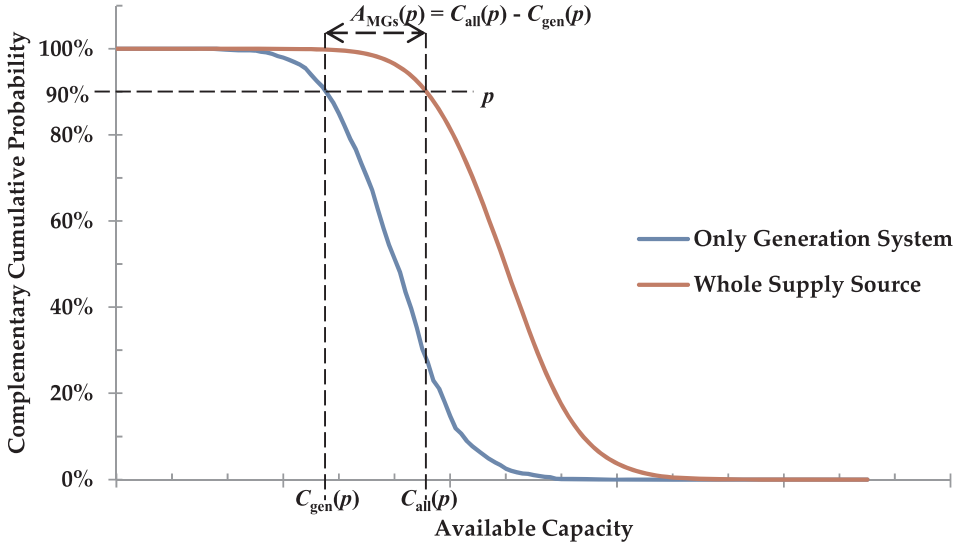

Fig. 4. Demonstration of evaluating the additional capacity of microgrids at system-level. The Whole Supply Source curve contains capacity contribution of both the main generation system and microgrids.

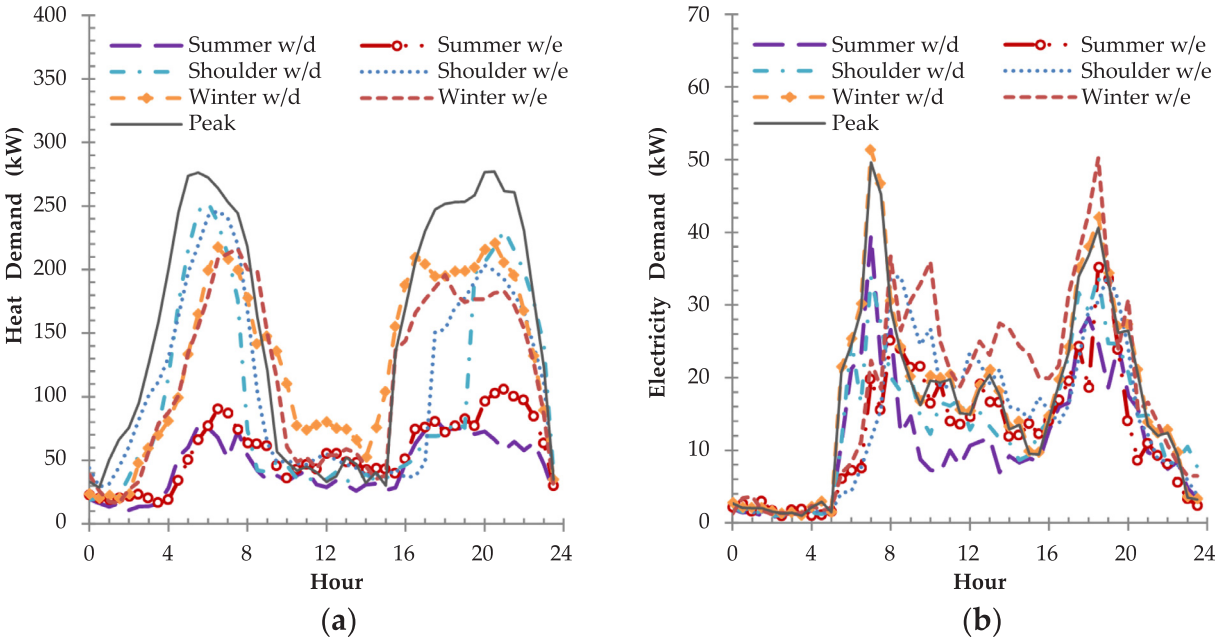

Fig. 5. Energy demand of 100 British semi-detached houses for seven typical days: (a) heat demand; (b) electricity demand.

Table 2
Parameters assumed for CHP unit, thermal energy storage, PV installation and batteries.

		MG1	MG2
CHP	Electricity capacity (kW_e)	51.4	–
	Electricity efficiency	37%	–
	Heat efficiency	47%	–
Thermal energy storage	Thermal capacity (kWh_{th})	210	–
PV panels	Capacity (kW)	–	275
Batteries	Power capacity (kW_e)	–	109.8
	Energy capacity (kWh_e)	–	65.9
	Roundtrip efficiency	–	90%

Table 3
Generation portfolio of the test british electricity system and average availabilities of different generation technologies.

Technology	Total capacity (GW)	Average capacity per generator (MW)	Average availability
Nuclear	9	1781	81%
CCGT	33.5	734	85%
Biomass	2.1	458	88%
Coal	16.2	1368	88%
Pumped Hydro	2.7	809	96%
Wind	12.9	–	–
Solar	4.2	–	–

microgrids. In other words, this paper does not aim to present results representing accurately the real system, but rather illustrative ones based on recognized resources that would be implemented in the real system. Ultimately, the objective is to present transparent results and discuss in a clear way the main distinctions among different reserve services and the main trends associated with the contributions from microgrids (including also the quantitative framework). Nonetheless, a large number of microgrids of each type is considered in the case study application focusing on the test British system (aggregation of 9046 MG1 and 15,272 MG2). Furthermore, the framework illustrated in Fig. 1 is sufficiently general to deal with any type of microgrids, which can be aggregated with others at the system-level/national-level.

As a further remark, the case study later extrapolates the contribution from the two representative microgrids (i.e., MG1 and MG2) to that from all microgrids to the main test British system. This implies for example that an identical profile of PV generation is considered for all the PV installation. This will add to the discrepancy between the numerical results in the paper and the actual contribution from these distributed energy resources. Nonetheless, the numerical results (though demonstrating an estimation of the contribution from microgrids at the system-level) can be further improved and become more realistic by using energy demand and PV generation profiles with actual spatiotemporal differences across the British electricity system.

4.1.2. Test British electricity system

A test British electricity system is adopted based on public data published by the British System Operator (i.e., National Grid [51]) and the system regulator (i.e., Ofgem [52]). Table 3 presents the generation portfolio of the test British electricity system in 2015 [51] and the corresponding average availability of the generation technologies. The detailed models of solar and wind generation at system-level have been described in [34] and [53], respectively. More specifically, the seasonal and geographical features of solar generation come from the models in [34] that correspond to the solar generation when modelled directly at a national level (i.e., modelling the aggregated solar generation of the test British system using historical solar irradiance at 11 representative locations as well as corresponding installed PV capacities across the British system [34]). It has to be highlighted here that this is different comparing the modelling of PV outputs of MG2 (which are modelled based on the solar irradiance of the aforementioned seven typical days and also included in the Annex), as described in the framework for modelling individual microgrids. This direct aggregation of solar generation at a national level is used in Section 4.3.2, where the contribution from PV installation is not via the form of microgrids. Meanwhile, the seasonal and geographical features of wind generation are based on the study in [53], where 39 representative onshore and offshore wind farms are used to model the aggregated wind generation of the test British system.

4.2. Electricity capacity contribution of an individual microgrid to reserve services

This section demonstrates the respective electricity capacity contribution of each of the two test microgrids as introduced in Section

4.1.1. The results focus on the contribution with various service durations. More specifically, the service duration (as defined in Section 2.2.1) varies from 1 to 5 h for traditional operating reserve, i.e., for security purposes. Afterwards, in order to highlight the difference between security-related and resilience-related services, prolonged service durations including 10 h, 15 h, 20 h and 24 h are studied with respect to the reserve services that may be required to enhance the system resilience to high impact low probability events.

4.2.1. Probabilistic capacity tables of MG1

Probabilistic capacity tables of MG1 with different service durations are presented as boxplots[3] in Fig. 6, while the available capacity duration curves are illustrated in Fig. 7. As seen in the figures, given a particular service duration, the electricity capacity contribution from MG1 varies from 0 to 51 kW depending on the starting time. It can be found that the longer the service duration, the more likely the service window would cover high levels of electricity demand inside MG1, and hence the less the contribution from MG1 to system-level reserve services.

More importantly, Figs. 6 and 7 demonstrate that though MG1's CHP unit is not oversized particularly for providing electricity capacity to upstream networks, there is a considerable amount of time throughout the year that MG1 has a considerable amount of electricity generation capacity surplus. This intrinsic flexibility of microgrids is properly captured here.

4.2.2. Probabilistic capacity tables of MG2

Similarly, with consideration of different service durations, probabilistic capacity tables and available capacity duration curves of MG2 are presented in Fig. 8 (in the form of boxplot) and 9, respectively. As seen in Fig. 8, the probabilistic capacity tables of MG2 distribute widely from 0 to 296 kW, while the majority of the electricity capacity contribution is within the range between 0 and 75 kW (as indicated by the boxes in Fig. 8).

Additionally, Fig. 9 clearly demonstrates that the available capacity duration curves of MG2 have widespread long and thin tails. This implies that high levels of electricity capacity contribution may be possible but the corresponding probability is low (also as indicated by the outliers "+" in Fig. 8). Though the installed PV capacity is considerably higher than the electricity peak demand (275 kWp compared with 51.4 kWe), the chance for PV panels to reach their peak generation is rare and the intermittency of PV generation makes the high electricity capacity contribution be possible only at particular times. This is fundamentally different from MG1, where the CHP unit can be dispatched according to the need of system.

Further, it can be seen that MG2 yields much lower electricity capacity contribution to reserve services for resilience purposes, i.e., those with service duration longer than 5 h. In addition, when Fig. 9 is compared with Fig. 7, it can also be found that the electricity capacity contribution of MG2 decreases much faster than that of MG1 following the increase of service duration. This is because, apart from the impact of internal electricity demand, MG2 is an energy-limited microgrid compared with MG1. More specifically, it is considered that MG1 has continuous supply of gas (i.e., energy unlimited), allowing its CHP unit to generate electricity as long as the accompanying heat production can be consumed or stored. In contrast, the batteries in MG2, as a key player in the service provision, are energy-limited (i.e., relying significantly on the energy stored at the beginning of a service), which may or may not be able to be charged by the variable PV generation (see Eq. (9)). The energy-limited feature of MG2 leads to the phenomenon observed in Fig. 9, i.e., the electricity capacity contribution from MG2 decreases drastically following the increase of service duration.

4.2.3. Comparison of MG1 and MG2 for reserve services based on guaranteed capacity

The guaranteed capacity is evaluated for MG1 and MG2 with the probability of 90% (other probability can be chosen as appropriate), as seen in Table 4 where the average electricity capacity contribution is also listed. Additionally, two operation strategies introduced in Section 2.3 ("Base" and "Res" Strategies) are also compared.

Generally, both the guaranteed capacity and the average contribution decline when the service duration increases. For instance, with regards to the services for security, the guaranteed capacity of MG1 decreases by 7 kW (from 19 kW to 12 kW) when the service duration increases from 1 h to 5 h; whereas, that of MG2 drops from 29 kW to 1 kW. This is attributed to the energy-unlimited feature of MG1 (i.e., assuming adequate supply of gas) and the energy-limited feature of MG2 (i.e., limited energy stored in batteries). Further, the support from a single microgrid to the reserve services featuring prolonged service duration (i.e., those over 5 h for resilience purposes) is very limited, such as for the service duration of 24 h MG1 presents a guaranteed capacity of 1 kW or an average contribution of 12.7 kW.

Moreover, when comparing the guaranteed capacity between "Base" and "Res" Strategies, it is found that MG1 exhibits the same level of guaranteed capacity; whereas, the guaranteed capacity of MG2 demonstrates a significant increase attributed to the reserve payment (i.e., £ 0.00451 per kW per hour). In other words, the reserve payment books electricity capacity headroom (particularly in MG2's batteries) in the planned operation of microgrids [9]. On the other hand, as the thermal energy storage in MG1 is oversized for energy arbitrage and heat supply [9], it has sufficient headroom regardless of the strategies.

4.3. Collective electricity capacity contribution at system-level

This section presents the case study application on the assessment of the collective electricity capacity contribution from microgrid across the network at system-level.

4.3.1. Aggregation of probabilistic capacity tables of microgrids

This section presents the aggregation of probabilistic capacity tables of microgrids using MG1 as example. A thousand identical MG1s are aggregated and their probabilistic capacity tables are shown in Fig. 10. These probabilistic capacity tables are mostly normally distributed. As seen in Fig. 10, a wider range of the probabilistic capacity table can be found for the minimum capacity surplus that can be contributed to reserve services lasting between 1 and 5 h (reliability-related), compared with that found for the minimum capacity surplus that can be contributed to reserve services lasting between 10 and 24 h (resilience-related). This means that the contribution from 1000 MG1s to short duration services depends more on the starting time of the reserve service than that to long-lasting services, when the starting time of the relevant service varies. In other words, the contribution to long-lasting reserve services (resilience-related) is mostly constrained by the internal energy consumption pattern as well as the energy-limited resources of those microgrids, rather than the starting time of the reserve service.

In addition, the corresponding guaranteed capacity of the considered group of microgrids (1,000 MG1s) is listed in Table 5, where the guaranteed capacity of a single MG1 is also presented. It can be observed that the guaranteed capacity of the considered group of MG1s is much higher than a thousand times of that of a single MG1, owing to the diversity inherent in their electricity capacity contribution (as these microgrids are assumed to be independent). More importantly, though a single microgrid fails to make a substantial contribution to the reserve

[3] For a clear illustration of the probabilistic capacity tables, Fig. 6 demonstrates these probabilistic capacity tables in the form of boxplot. The bar in the middle of the box is the median value, while the edges of the box are the 25th and 75th percentiles. The whiskers extend to the values that are covered by the *3-sigma* rule (i.e., if the data were normally distributed, 99.7% of the data would be within the whiskers), whereas the most extreme values (or outliers) are represented by "+" outside the whiskers. The same standard is applied to Fig. 8.

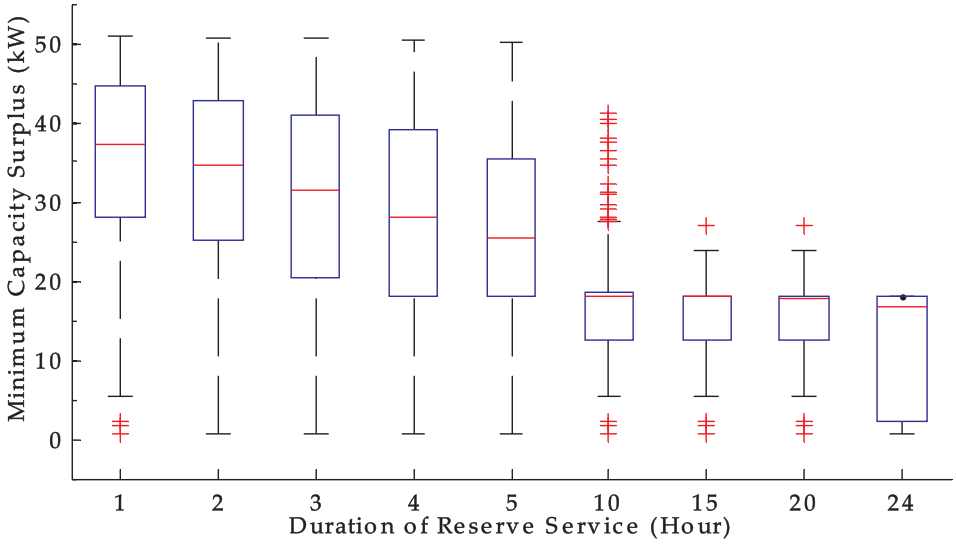

Fig. 6. Probabilistic capacity tables of MG1 presented as boxplots with consideration of various durations of reserve service.

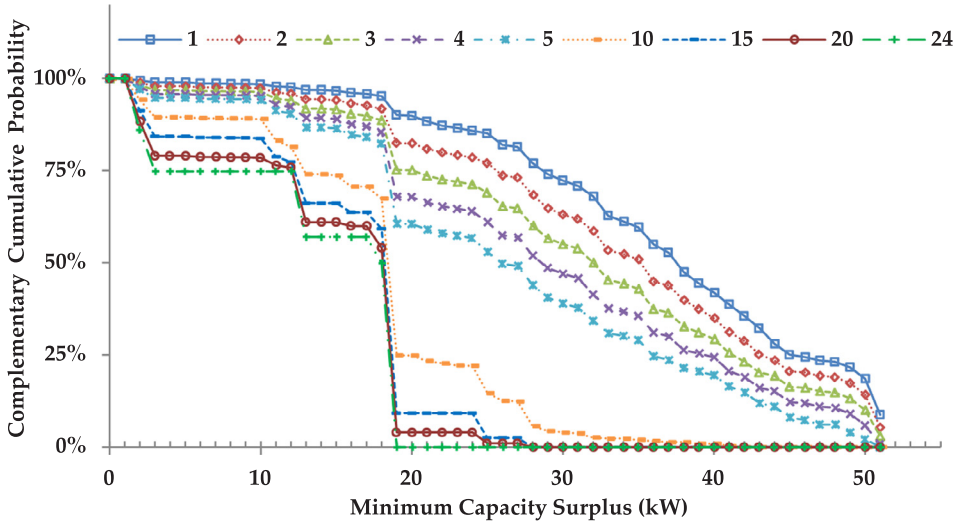

Fig. 7. Available capacity duration curve of MG1 with consideration of various durations of reserve service.

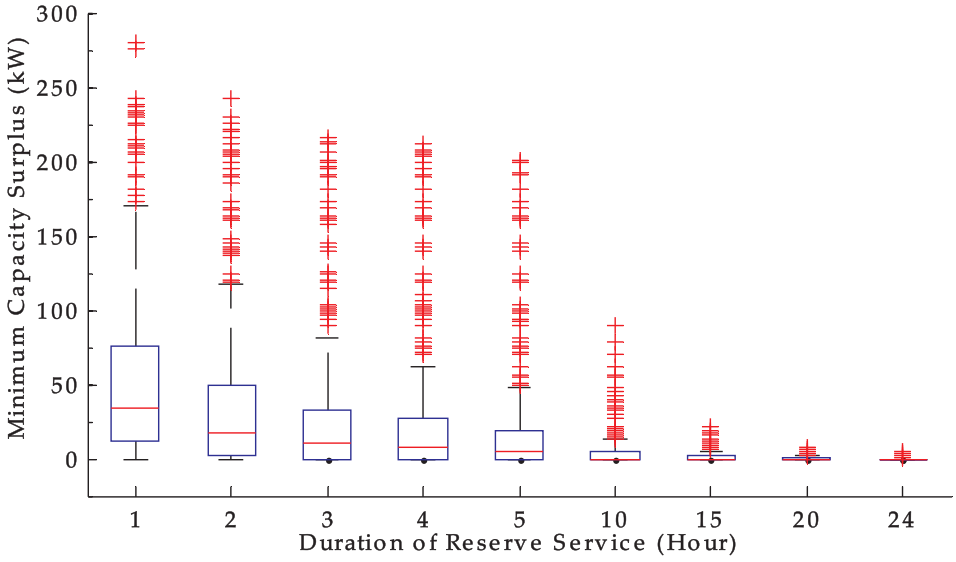

Fig. 8. Probabilistic capacity tables of MG2 presented as boxplots with consideration of various durations of reserve service.

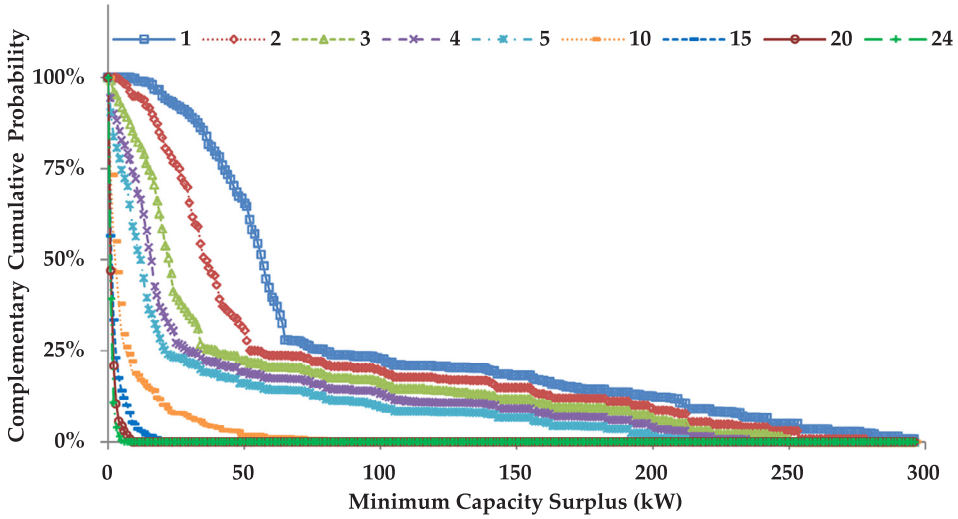

Fig. 9. Available capacity duration curves of MG2 with consideration of various capacity service windows.

Table 4
Guaranteed capacity with a probability of 90% and average capacity contribution evaluated for MG1 and MG2 under different scheduled operation strategies and different durations of reserve service.

Microgrid	Strategy	Metric	Length of service window (h)								
			1	2	3	4	5	10	15	20	24
MG1	Base & Res	Guaranteed capacity (kW)	19	18	16	12	12	2	2	1	1
		Average (kW)	36.1	33.4	31.0	28.6	26.3	17.2	14.7	13.5	12.7
MG2	Base	Guaranteed capacity (kW)	0	0	0	0	0	0	0	0	0
		Average (kW)	61.7	47.2	38.6	31.6	25.4	6.2	1.7	0.7	0.4
	Res	Guaranteed capacity (kW)	29	15	6	2	1	0	0	0	0
		Average (kW)	83.1	63.4	48.2	37.9	29.8	6.8	2.0	0.9	0.6

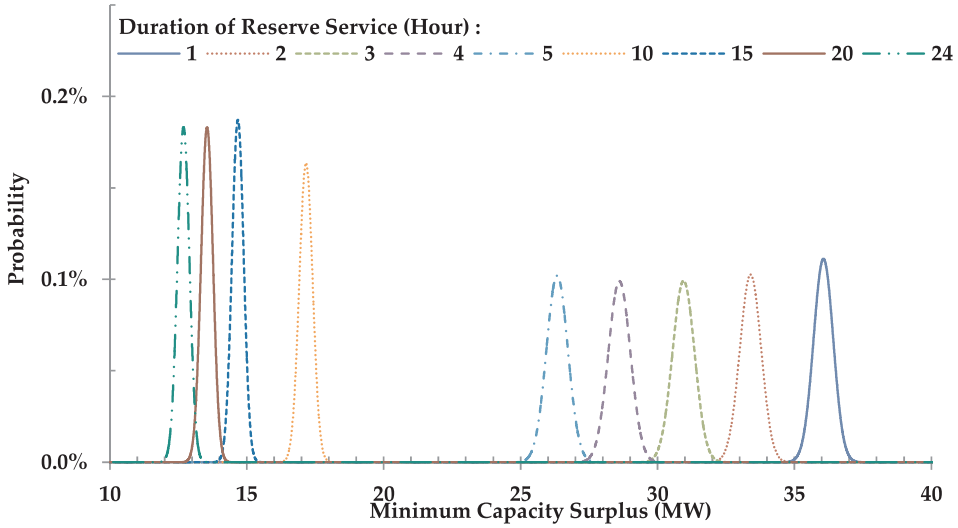

Fig. 10. Aggregated probabilistic capacity tables of one thousand identical MG1s with the capacity interval of 1 MW.

Table 5
Guaranteed capacity evaluated for a group of microgrids with a probability of 90%.

Duration of reserve service (h)	1	2	3	4	5	10	15	20	24
1000 MG1s (MW)	36	33	30	28	26	17	14	13	12
A Single MG1 (kW)	19	18	16	12	12	2	2	1	1

services for resilience, a group of microgrids, on the other hand, can in fact provide a significant amount of available capacity at system-level to enhance system resilience to extreme events needing prolonged restoration time. For instance, the guaranteed capacity of 1000 MG1 is 12 MW for a service duration of 24 h, whereas that of a single MG1 is merely 1 kW (see Table 5), demonstrating a significant improvement in the provision of security and resilience services associated with the aggregation of microgrids.

4.3.2. Assessment of additional available capacity

This section evaluates the additional available capacity of a group of microgrids in the system under two distinct scenarios, which are introduced as follows. According to National Grid [33], the total installation of distributed and small-scale CHP units is 465 MW in 2016. In this light, the first scenario (referred to as S1) considers that all the distributed and small-scale CHP units operate as MG1 without loss of generality, leading to 9046 identical MG1s (i.e., 465 MW divided by 51.4 kW).

In S1, the probabilistic capacity table of the test British electricity generation system is created based on all the generation technologies as listed in Table 3, according to the approach in Section 3.2.2. Meanwhile, the aggregated probabilistic capacity table of the group of MG1s (with 465 MW of CHP units) is created through convolution of the probabilistic capacity table of MG1 in Fig. 6, separately for all service durations from 1 to 24 h. A new probabilistic capacity table of both the test British electricity generation system and these MG1s can be obtained separately for all service durations from 1 to 24 h. Eventually, the available capacity duration curve of the test British electricity generation system and that of both the test British electricity generation system and these MG1s can be developed, as shown in Fig. 11 for the duration of 1 h (i.e., for security purposes).

As seen in Fig. 11, the electricity capacity contribution from these microgrids with a total CHP capacity of 465 MW, considering a probability of 99% [45], can provide an additional available capacity of 319 MW (68.6% of the total CHP capacity) to enhance system security via reserve services lasting 1 h. Additionally, their contribution to other reserve services (both security and resilience purposes) is presented in Table 6 in the form of *additional available capacity* considering a probability of 99%. Despite the observed declining trend of their contribution to the system available capacity, these microgrids with a total CHP capacity of 465 MW can for instance provide an additional available capacity of 149 MW to enhance system resilience via reserve services with the duration of 10 h, i.e., 32% of the total CHP capacity, while the contribution to resilience-related reserve service lasting for 24 h is 109 MW (which is significant considering the supporting duration).

On the other hand, as seen in Table 2, the total solar capacity is 4.2 GW; and in fact according to National Grid [51], the majority of the solar capacity corresponds to the installation of PV panels in distribution networks. Therefore, the second scenario (referred to as S2) considers that all the solar capacity is adopted to form microgrids represented by MG2. This corresponds to approximately 15,272 identical MG2s (i.e., 4.2 GW divided by 275 kW).

Table 6
Contribution to system available capacity from a group of microgrids with a total CHP capacity of 465 MW.

Duration of reserve service (h)	1	2	3	4	5	10	15	20	24
Additional available capacity considering a probability of 99% (MW)	319	294	273	252	232	149	127	115	109

Unlike the assessment shown earlier, the probabilistic capacity table is built for the test British electricity generation system excluding the solar generation. This is because all the solar installation in S2 belongs to microgrids. Meanwhile, the aggregated probabilistic capacity table of the group of MG2s is created by convolution of the probabilistic capacity table of MG2 as seen in Fig. 8, separately for all service durations from 1 to 24 h. Eventually, the available capacity duration curve of the test British electricity generation system without solar generation and that of the one with additional electricity capacity contribution from all the microgrids are presented as an example in Fig. 12 for the duration of 1 h (i.e., for security purposes).

In Fig. 12, an additional available capacity of 1,247 MW can be contributed by microgrids with a PV installation of 4.2 GW for the purposes of enhancing system security via reserve services with duration of 1 h (also seen in the figure that the direct contribution from the PV installation is only 258 MW). Similarly, their contribution to other reserve services including both security-related and resilience-related are presented in Table 7. As seen in the table and most importantly, the contribution from a single MG2 to resilience (via reserve services with a supporting duration longer than 5 h) is extremely limited (close to zero as seen in Table 4); however, according to Table 7 the collective contribution from a group of MG2s at system-level can reach to 102 MW via reserve services with duration of 10 h (though not as significant as their contribution to security). Nevertheless, in order to deliver this level of additional available capacity, the system will have a battery installation of approximately 1.6 GWh.

4.3.3. Impact of the level of microgrid integration on contribution to reserve services

As mentioned in Section 1.1, the level of microgrid integration is expected to increase significantly in the future [30]. In this light, the following studies are carried out focusing on the increasing penetration

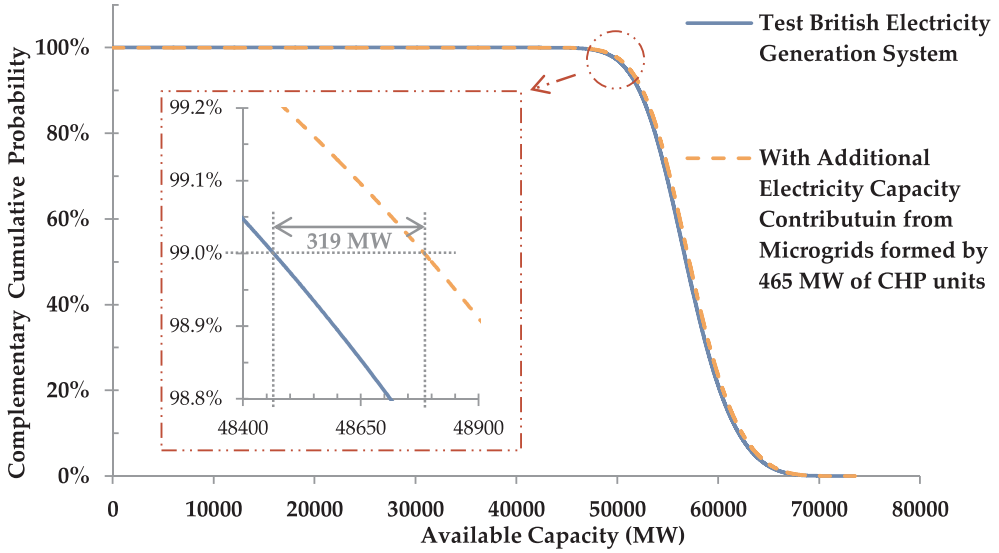

Fig. 11. Contribution to security via reserve services with duration of 1 h: available capacity duration curves of the test British electricity generation system and all the electricity supply resources including microgrids formed by 465 MW of CHP units; as well as the assessment of the corresponding additional available capacity.

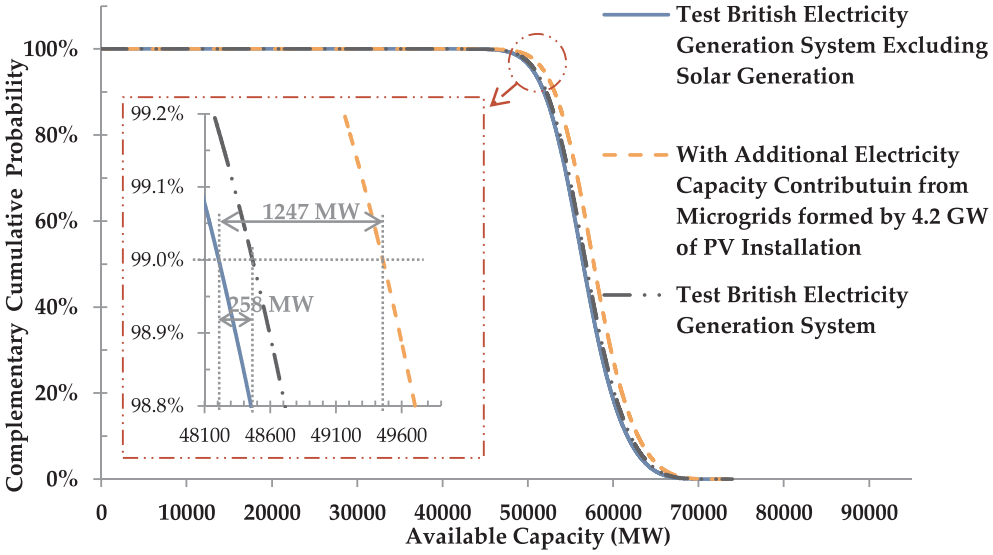

Fig. 12. Contribution to security via reserve services with duration of 1 h: available capacity duration curves of the test British electricity generation system excluding solar generation and all the electricity supply resources including microgrids formed by 4.2 GW of PV installation; as well as the assessment of the corresponding additional available capacity.

Table 7
Contribution to system available capacity from a group of microgrids with a total PV capacity of 4.2 GW.

Duration of reserve service (h)	1	2	3	4	5	10	15	20	24
Additional available capacity considering a probability of 99% (MW)	1247	953	724	569	446	102	28	14	14

of distributed CHP units and PV panels in the British system, which is represented by the two representative types of microgrids (i.e., MG1 and MG2, respectively).

More specifically, the penetration level of CHP units is analyzed by varying it from 500 MW to 2.5 GW with steps of 500 MW (as mentioned in Section 1.2 the total CHP capacity will reach 2,348 MW by 2040 [33]). Fig. 13-(a) demonstrates the increase in the additional available capacity following the increase of CHP penetration level. It can be seen clearly that the additional available capacity increases linearly when CHP penetration increases. More importantly, it is also found that the incremental rate of the additional available capacity via reliability-related services (with service duration from 1 to 5 h) is much higher than that of the additional available capacity via resilience-related services (with service duration over 5 h). This implies that the additional system-level contribution to resilience provision would be lower compared to reliability provision, when more microgrids are formed and participate in providing reserves services. Similarly, the same trend is found in Fig. 13-(b), where the results are for microgirds with PV installation (which is varied from 5 GW to 16.5 GW according to the projection in [33]). Due to the energy-limited feature of batteries, the increase in the additional available capacity via resilience-related services (with service duration over 5 h) is also very limited (extremely low incremental rate of additional available capacity under service duration longer than 10 h in Fig. 13-(b)) even though the number of microgrids with PV installation (represented by the penetration level of PV) increases rapidly.

In summary, these results provide valuable information to the policy makers to obtain a more comprehensive understanding of the additional contribution from integrating more microgrids to the main electricity grid, i.e., the corresponding additional contribution depends significantly on the duration of reserve services. In other words, the additional contribution to reliability provision is different from that resilience provision, though from the same number of additional microgrids. According to Fig. 13, integrating more microgrids would present higher value to reliability provision than to resilience provision.

4.4. Discussion and limitation of the case study application

Specific case study applications have been carried out on two representative microgrids and a test British electricity generation system. The two representative microgrids are fundamentally distinct to each other, i.e., the first one (MG1) represents those with controllable generation resources (such as distributed CHP units or diesel generators), whereas the second one (MG2) exemplifies the microgrids with intermittent renewable generation (uncontrollable as PV panels) and electrical energy storage. It can be seen from the results that the electricity capacity contribution from MG1 decreases when the service duration increases due to the fact that the longer the service duration the higher the likelihood that the service window would cover the electricity peak demand of MG1, when the capacity surplus is naturally reduced. On the other hand, it can also be observed that the electricity capacity contribution from MG2 can be higher than that from MG1 when the service duration is short (e.g., one hour); however, it drops significantly faster when the service duration increases (the guaranteed capacity with the probability of 90% becomes zero when the capacity service duration is over 5 h). This is mainly because, in addition to the constraint imposed by the internal energy demand, the energy stored in batteries can only sustain the supply for certain amount of time. Additionally, in the light of the energy-limited feature of batteries, the two sets of studies analyzed for MG2 clearly suggest that proper incentives (or market structures) can make a substantial difference, i.e., the guaranteed capacity of MG2 would be zero if there were no incentive for reserve service.

The aforementioned results clearly demonstrate how, though individually constrained by the power and/or energy capacities of internal resources, aggregation of various microgrids can significantly improve their contribution to both reliability and resilience at the system-level, far beyond the simple summation of the individual contributions, demonstrating a clear synergic effect. More specifically, from the British case study applications, coordination of distributed and small-scale CHP units in the form of microgrids can contribute a substantial proportion (68.6%) of their installed capacity to the available generation capacity of the system through one-hour services. Even more importantly, the contribution from PV to the system's available capacity is much higher (approximately 5 times higher) when the distributed PV panels are combined with batteries and are operated in the form of microgrids, compared with the contribution made solely by PV panels. These results can be applied by local aggregators to participate in reserve markets as well as be considered by policy makers and system regulators to introduce new markets or other arrangements to implement new "resilience" services.

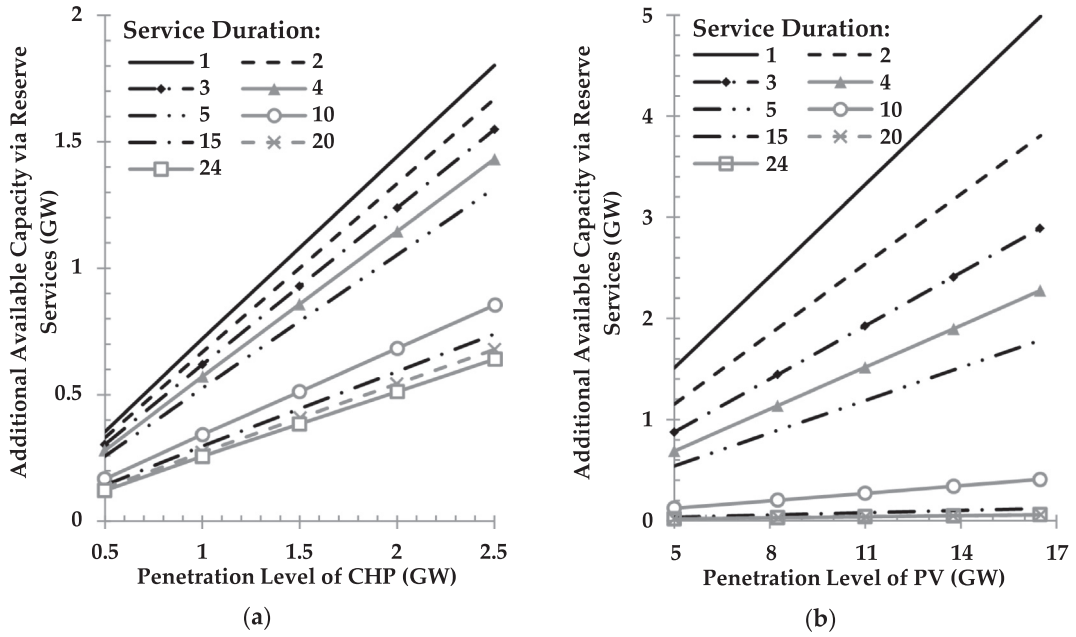

Fig. 13. Increase in the additional available capacity through providing reserve services (for both reliability and resilience purposes) owing to the increase in the penetration level of microgrids: (a) the microgrids with CHPs represented by MG1 and (b) the microgrids with PV panels and batteries represented by MG2.

Further, studies focusing on the impact of increasing penetration levels of microgrids are also carried out in the context of the British system. It is found that in general integrating more microgrids presents different additional values for reliability provision and resilience provision at the system-level.

However, the numerical results obtained in the case study application have to be understood in the context of the following assumptions to enable transparent conclusions, such as:

a) The proposed optimization considers perfect forecasting, though uncertainties in energy demands and renewable generation are modelled using seven typical days;
b) Full cooperation of microgrids is considered and achieved by cost-minimizing, while in reality the actual contribution from microgrids heavily relies on their cooperation;
c) Various types of microgrids can be formed in the context of the British system, not being limited to the two specific types of microgrids simulated and analyzed in detail earlier (though they are representative in terms of the resources they have);
d) Extrapolating the contribution from a single MG2 to that from a number of MG2s at the level of the test British system implies that the spatiotemporal diversity of solar irradiance and temperature cannot be captured by the relevant results;
e) Dependency among microgrids can affect their aggregated contribution to the main electricity system. Independency is assumed for the case study application, in the light of the large number of microgrids aggregated at the system-level and their inherent diversity.

Nonetheless, the aforementioned impacts could be captured through more complex modelling approaches as well as more realistic scenarios of microgrids, and this is suggested for future investigations.

5. Conclusions and future work

This paper has introduced a framework for quantifying the system-level electricity capacity contribution from microgrids to various reserve services, including prolonged support following potential rare, catastrophic events. Probabilistic capacity tables have been defined in order to take account of multiple sources of uncertainty related to both the operation of the microgrids and the occurrence of unfavorable events in the main electricity grid. An optimization model has been proposed to determine microgrid's operation in real time by maximizing the electricity capacity that can be provided by a microgrid in a particular scenario when a reserve service is exercised. The proposed framework uses service duration to differentiate the reserve services for security purpose from those for resilience purpose. Hence, we have also defined a new type of reserve service with prolonged service duration, which is complementary to the traditional operating reserves featuring short supporting duration. The concept of guaranteed capacity has been extended to indicate the level of electricity capacity contribution from microgrids with a specific probability (or confidence), which quantifies the contribution from the microgrid's point of view. Additional available capacity has been defined to quantify the contribution from the generation system's point of view.

As key findings we showed that due to the constraints imposed by the internal energy consumption of a microgird as well as the energy limitation of storage, a single microgrid can contribute much more to reserve services with short supporting durations (for reliability provision), compared with its contribution to those requiring prolonged supporting durations (which are for resilience provision). However, in spite of the individual capacity and/or energy limitations, aggregation at the system-level of various microgrids can significantly improve the contribution to both reliability and resilience, far beyond the simple summation of the individual contributions, demonstrating a clear synergic effect. Generally, integrating more microgrids presents higher additional value to reliability provision than to resilience provision at the system-level. The results focusing on the penetration level also demonstrate that the proposed framework can inform policy makers and regulators on the strategic role of microgrids for energy system planning and policy developments, and assist them to design appropriate ancillary services and markets not only to enhance system reliability (as current reserve services worldwide do) but also its resilience.

For future application of the proposed framework, various types of microgrids for the British system (representing the actual diversity of resources in the British system) will be modelled and their aggregated contribution to reserve services will be quantified using the presented framework, in order to provide more realistic results and implications to assist specific planning decisions on the British system development.

Future work will focus on developing an economic framework such that the economic value of the electricity capacity contribution from microgrids can be properly quantified. This could also further influence the development of microgrids in terms of their individual design to allow new business cases, for example by oversizing them for the purpose of providing capacity services to upstream networks. Additionally, it is also essential to thoroughly investigate how and to what extent the cooperation of microgrids can impact their contribution to system-level reliability and resilience via various reserve services, which will be a critical part of additional research built on the work carried out in this paper. Similarly, the quantification of to what extent dependency among microgrids (such as dependency of resource availabilities and dependency due to responses to the system price signals) has to be conducted to demonstrate a complete picture of microgrids's contribution at the system-level to reserve services.

Acknowledgments

The presented research work in this paper was developed with the contribution and within the scope of the EPSRC funded projects "Disaster Management and Resilience in Electric Power Systems" (EP/N034899/1), "MY-STORE" (EP/N001974/1) and "Techno-Economic framework for Resilient and Sustainable Electrification (TERSE)" (EP/R030294/1), which the authors would like to acknowledge. Additionally, Dr. Moreno would like to gratefully acknowledge the financial support from the Complex Engineering Systems Institute (through the grants including CONICYT-PIA-FB0816 and ICM P-05-004-F), the Energy Center at the University of Chile and the Conicyt-Chile (through the grants including Fondecyt/1181928, Newton-Picarte/MR/N026721/1, and SERC Fondap/15110019) as well as the EPSRC-UK project "Energy Storage for Low Carbon Grids" (EP/K002252/1).

Appendix A

(see Tables 8 and 9).

Table 8
Database of typical day temperature and PV output.

Time	Summer w/d		Summer w/e		Shoulder w/d		Shoulder w/e		Winter w/d		Winter w/e		Peak	
	Temp (°C)	PV (kW)	Temp (°C)	PV (kW)	Temp (°C)	PV (kW)	Temp (°C)	PV (kW)	Temp (°C)	PV (kW)	Temp (°C)	PV (kW)	Temp (°C)	PV (kW)
00:00	15.3	0	14.6	0	2.2	0	4.7	0	6.7	0	5.8	0	0.7	0
00:30	15	0	14.1	0	2	0	4.5	0	6.5	0	5.7	0	0.7	0
01:00	14.9	0	13.7	0	1.9	0	4.1	0	6.4	0	5.9	0	0.7	0
01:30	14.7	0	13.5	0	1.9	0	3.9	0	6.4	0	6	0	0.7	0
02:00	14.5	0	13.5	0	1.9	0	3.5	0	6.3	0	6	0	0.6	0
02:30	14.3	0	13.6	0	2.2	0	3.1	0	6.3	0	6	0	0.7	0
03:00	13.8	0	13.2	0	2.2	0	2.7	0	6.5	0	6.2	0	0.7	0
03:30	13.9	0	12.8	0	2.1	0	2.3	0	6.4	0	6.3	0	0.4	0
04:00	13.6	0	12.5	0	2.1	0	1.9	0	6.2	0	6.3	0	0.3	0
04:30	13.6	0	12	0	2.1	0	1.6	0	6.2	0	6.2	0	0.4	0
05:00	13.4	0	11.8	0	1.9	0	1.3	0	6.2	0	6.1	0	0.6	0
05:30	13.1	0	11.5	0	1.8	0	1	0	6.2	0	6	0	0.3	0
06:00	12.7	0	11.4	0	1.8	0	0.4	0	6.1	0	6	0	0.4	0
06:30	12.4	2.7	11.3	0.3	2	0	0.2	0	6.1	0	6	0	0.8	0
07:00	12.4	12	11.2	5.9	2.2	0.5	0	0.1	6.3	0	6.1	0	1.1	0
07:30	12.8	18.5	11.8	21	2.4	6.2	−0.1	2.8	6.3	0	6.1	0	1.1	0
08:00	13.3	42.9	12.8	34.6	2.7	20.9	0.5	10.5	6.3	0	5.8	0	1.1	0.1
08:30	14.1	68.6	13.5	57.3	3	34.2	1.3	22.9	6.4	0.4	5.6	0.1	0.9	1.2
09:00	14.7	86	14.2	86.5	3.3	52.6	2.1	38.7	6.5	0.4	5.6	1.5	0.7	3.9
09:30	15.1	130.2	14.9	133.8	3.6	77.6	2.9	57.1	6.7	0.9	5.5	3.5	0.9	13.3
10:00	15.8	97	15.1	93	4	120.2	3.5	75.4	6.9	2.5	5.6	9.8	1.4	21.7
10:30	15.7	136.3	15.5	178.2	4.8	172.8	4.6	91.7	7.2	4.3	6.2	18.4	1.5	27.6
11:00	16.2	151	16	190.6	5.1	171.8	5.1	107.3	7.5	5.9	7.1	25.6	1.9	33.9
11:30	16.3	133.2	16.1	234.7	5.5	193.3	5.8	118.5	7.4	6.4	7.4	30.7	1.5	30.8
12:00	16.5	208.8	15.9	148.6	6	228.1	6.3	125	7.2	5.6	7.7	28.6	1.7	32.4
12:30	16.8	187.8	16	249.4	6.1	238.9	6.8	126.3	7.2	7.7	7.9	31	1.6	33.1
13:00	16.9	221.6	16.2	180	6.3	245.1	7.4	125.8	7.4	6.8	7.9	21.4	1.8	32.1
13:30	17.3	255.6	15.9	230.9	6.5	241.8	8.1	128.8	7.6	4.6	8.2	21.9	1.4	23.8
14:00	17.3	155.2	16.5	246.2	6.6	198.2	8.8	108	7.5	2.9	8.5	20	1.4	16.9
14:30	17.7	215.5	16.1	184.7	6.5	211.2	8.9	88.7	7.5	1.8	8.4	9.4	1.4	8.6
15:00	17.7	174.6	16	154.5	6.9	207.4	8.7	72.2	7.6	0.6	8.2	2.7	0.9	3.7
15:30	18	198.6	16.4	208.5	6.8	159	8.7	53.4	7.6	0	7.7	0	0.8	0.1
16:00	18	179.6	16.2	158.3	6.8	130.1	8.1	30.2	7.3	0	7.3	0	0.7	0
16:30	18.2	158.7	16.3	156	6.6	114	7.9	19.7	7.1	0	7	0	0.7	0
17:00	18.4	110.9	16.6	127.2	6.9	98.9	7.7	6.7	7	0	6.8	0	0.8	0
17:30	18	58.6	16.3	98.1	6.7	69.9	7.3	0	6.9	0	6.6	0	0.8	0
18:00	17.9	59.6	16.2	71.7	6.6	37.7	7.4	0	6.8	0	6.6	0	0.7	0
18:30	17.9	48.3	15.8	24.2	6.4	18.8	7.3	0	6.9	0	6.6	0	0.8	0
19:00	18.1	33.8	15.5	13.3	5.8	6.3	7.2	0	6.8	0	6.8	0	0.7	0
19:30	18	14.3	15.2	0.6	5.4	0	7	0	6.8	0	7.2	0	0.3	0
20:00	17.5	0.3	15.2	0	4.9	0	6.5	0	6.7	0	7	0	0.4	0
20:30	16.9	0	14.9	0	4.5	0	6.2	0	6.6	0	6.9	0	0.7	0
21:00	16.6	0	14.5	0	4.2	0	6	0	6.6	0	6.9	0	0.6	0
21:30	16.4	0	14.3	0	3.7	0	5.9	0	6.7	0	6.8	0	0.2	0
22:00	15.9	0	14.3	0	3.3	0	5.5	0	6.8	0	6.6	0	−0.1	0
22:30	15.5	0	14	0	2.9	0	4.9	0	6.7	0	6.7	0	−0.1	0
23:00	15.2	0	13.8	0	2.6	0	3.8	0	6.8	0	6.8	0	−0.1	0
23:30	15	0	13.8	0	2.4	0	3.3	0	6.6	0	6.7	0	−0.3	0

Table 9
Typical day profiles of energy demands (electricity and heat) in kW.

Time	Summer w/d		Summer w/e		Shoulder w/d		Shoulder w/e		Winter w/d		Winter w/e		Peak	
	Elec	Heat	Elec	Heat	Elec	Heat	Elec	Heat	Elec	Heat	Elec	Heat	Elec	Heat
00:00	1.9	19.5	2.1	22.8	2.2	19	2.9	43.9	2.8	23.5	1.3	38.8	2.7	33.2
00:30	1.4	16.4	2.6	20	1.5	20.8	2.2	29.1	2.1	20.4	3.4	26	2.1	28.6
01:00	1.5	13.3	1.6	19.1	1.9	19.7	1.4	31.7	2.1	22.4	3.6	17.3	2	50.4
01:30	1	16.2	3	20.4	1.2	22	1.5	44.6	2.1	20	1.7	16.5	2	66.1
02:00	0.8	10.8	1.7	21.7	1	36.9	1.7	60.6	1.6	23.4	1.2	27.1	1.6	75.5
02:30	1.1	13.5	0.9	23.3	1	54.5	0.8	82.2	1.3	47.9	1.4	33.3	1.3	95.2
03:00	1.3	13.9	1.8	20.3	1.5	56.8	1.7	101.4	1.5	59.5	1.1	57.2	1.4	126.4
03:30	1.5	16.1	1.9	16.7	0.7	76.6	0.9	111.9	1	69.8	1.4	79.1	1	159.2
04:00	1.1	28.2	1	19	1.4	115.7	1.9	130.9	2.3	81	2.3	87.6	2.2	200.2
04:30	1.1	53	1.1	34.3	1.2	173.2	1.3	163.7	3	99.2	1.7	101	2.9	245.3
05:00	2.1	60.2	1.6	50.3	1.7	215.5	1.6	197.8	1.5	133.6	1.9	134.4	1.5	273.7
05:30	10.9	76.8	6.1	65.9	11.1	245.9	4.2	219.1	21.5	165	6.8	155	20.8	276.3
06:00	21.2	75.7	7.2	77	25.1	252.9	4.4	242.2	25.4	199.4	8.3	179	24.5	272.4
06:30	23	68.1	7.5	90.4	16.4	237.3	7.6	246.2	30.2	217.7	11.2	208.2	29.2	264.2
07:00	39.6	51.6	19.8	86.9	33.7	211.9	11.5	240.5	51.3	208.3	22.4	212.6	49.6	253.2
07:30	21.9	72.8	15.5	74.2	27.3	176.5	15.6	219.8	46.7	199.7	18.4	216.6	45.2	244.5
08:00	26.6	54.2	25.1	63.6	20	73.9	33.7	168	30.6	177.6	36.7	200.3	29.5	218.1
08:30	12.3	41.9	23.9	62.9	18.1	42	33.9	103.5	24.2	141.5	26.5	198.4	23.4	162.7
09:00	14.7	34.4	21.4	61.2	20.2	40.8	28.9	63.8	20.2	147.6	30.6	149.6	19.5	120.5
09:30	8.8	38	21.6	45.7	14.6	49.2	24.5	48.5	16.8	135.9	32.9	113.5	16.2	56.9
10:00	7.3	33.7	16.5	36	12.2	45.7	26.8	49.4	20.2	110.4	36	60.6	19.6	48.7
10:30	6.9	38.3	19.3	42.8	16.6	35.7	18.7	47.5	20	77.2	25	49.1	19.3	41.9
11:00	10	41.8	14	46.7	16.1	33.9	18.8	46.6	20.4	73.9	21	52.3	19.8	45
11:30	7.8	30.8	13.6	43	17	37.1	18.7	51.8	15.6	77.9	18.8	43.8	15.1	40.7
12:00	10.6	28.8	14.6	55.3	12.8	35.1	23.6	54.9	15.4	80.1	21.6	54.1	14.9	32.9
12:30	11.2	34.2	19.1	55.3	15.3	41	22	49.9	19	75.3	25	54.1	18.4	37.4
13:00	11.7	30.8	16.6	48.9	13.3	33.9	19.2	46.9	21.1	74.3	23.1	58.9	20.4	52.1
13:30	7	25.9	16.6	48.2	11.6	34	21	43.9	18.1	66.2	27.5	55.8	17.5	47
14:00	9.2	31	11.9	42.5	11.1	39	16	38.3	13.3	52.4	26.7	45.3	12.9	32.3
14:30	8.3	31.7	12.1	43.5	8.7	34.2	15.6	38.9	14	75.8	24.3	35.5	13.5	40.7
15:00	8.9	26.5	13.7	43.1	9.4	35.3	14.4	36.6	9.9	104.1	23.1	38.1	9.5	30.1
15:30	8.5	28.6	12.2	39.7	12.5	42.7	17.3	43.3	9.7	155.3	20	136.8	9.4	135
16:00	12.7	47.6	14	51.2	14.1	46.3	15.4	36.3	14.7	187.8	19.9	143.9	14.2	170.3
16:30	16	63.3	16.9	74.4	18.3	51.6	13.7	37.8	19.8	209.6	21.7	166.1	19.1	206.9
17:00	16.5	73.6	19.5	76	23	69.2	16.2	48.5	24.2	204.2	31.5	176.6	23.4	230.4
17:30	25.7	82.1	24.3	80.4	31.6	69.2	22.5	151	35.1	194.5	37	185.8	33.9	247.3
18:00	28.2	73.9	18.6	72	29.2	69.8	29.3	153	38.1	194.9	42.7	195.7	36.8	251.9
18:30	24.8	74.8	35.2	76.9	34.1	80.6	30.4	170	42	198.6	50.2	181.2	40.6	253
19:00	18.6	75.4	33.5	82.6	24.7	75.7	34.3	177.6	34.4	198.7	34.1	174.5	33.2	253.4
19:30	24.5	70.5	23.8	77	24.6	196.7	30.6	190.2	27.1	201.7	24	176.7	26.2	258.7
20:00	17.5	72.7	14.1	96.4	20.7	205.7	24	203.4	27.4	215.8	30.7	176.8	26.4	276.5
20:30	15.7	66.4	8.6	102.8	14.7	217.2	14.4	199.2	21.1	220.8	15.5	181.6	20.4	277.1
21:00	9.7	58.1	10.9	105.7	14.8	231.1	12.1	192.2	13.9	205.7	16.6	182.7	13.4	261.6
21:30	9.2	64.5	9.3	100.3	12.3	215.2	8.7	180.7	12.4	195.7	13.7	171.7	12	260.9
22:00	7.4	57.8	8.1	97.4	7.9	199	8.4	166.9	12.9	167.6	10.7	153.7	12.4	230.8
22:30	8.4	63.9	5.6	84.5	8.7	174.2	8	139.4	9.7	132.1	8.3	126.1	9.4	176.5
23:00	4.8	46.9	3.3	63.5	10.5	140.2	5.9	110.5	3.6	89.2	6.4	85.9	3.5	123.2
23:30	3.4	25.2	2.4	30	7.7	39.3	3.8	33.9	3.3	34.9	6.5	29.7	3.2	35.2

References

[1] The Paris Agreement, United Nations, Paris, France, 2015, pp. 1–27.
[2] Good N, Karangelos E, Navarro-Espinosa A, Mancarella P. Optimization under uncertainty of thermal storage-based flexible demand response with quantification of residential users' discomfort. IEEE Trans Smart Grid 2015;6:2333–42.
[3] Panteli M, Mancarella P. The grid: stronger, bigger, smarter? Presenting a conceptual framework of power system resilience. IEEE Power Energy Mag 2015;13:58–66.
[4] Good N, Martinez Cesena EA, Mancarella P. Ten questions concerning smart districts. Build Environ 2017;118:362–76.
[5] Mancarella, P, Andersson G, Pecas-Lopes JA, Bell KRW. Modelling of integrated multi-energy systems; drivers, requirements, and opportunities. In: Proceedings of the 2016 IEEE power syst comput conf, Genoa, Italy, 20–24 June 2016. p. 1–22.
[6] Mancarella P. MES (multi-energy systems): an overview of concepts and evaluation models. Energy 2014;65:1–17.
[7] Capuder T, Mancarella P. Assessing the benefits of coordinated operation of aggregated distributed multi-energy generation. In: Proceedings of the 2016 IEEE power syst comput conf, Genoa, Italy, 20–24 June 2016. p. 1–7.
[8] Good N, Martinez Cesena EA, Zhang L, Mancarella P. Techno-economic and business case assessment of low carbon technologies in distributed multi-energy systems. Appl Energy 2016;167:158–72.
[9] Martinez Cesena EA, Good N, Syrri AL, Mancarella P. Techno-economic and business case assessment of multi-energy microgrids with co-optimization of energy, reserve and reliability services. Appl Energy. 2018;210:896–913.
[10] Neyestani N, Yazdani-Damavandi M, Shafie-khah M, Chicco G, Catalao JPS. Stochastic modeling of multi-energy carrier dependencies in smart local networks with distributed energy resources. IEEE Trans Smart Grid 2015;6:1748–62.
[11] Mancarella P, Chicco G. Real-time demand response from energy shifting in distributed multi-generation. IEEE Trans Smart Grid 2013;4:1928–38.
[12] Lin Y, Bie Z. Tri-level optimal hardening plan for a resilient distribution system considering reconfiguration and DG islanding. Appl Energy 2018;210:1266–79.
[13] Ding T, Lin Y, Bie Z, Chen C. A resilient microgrid formation strategy for load restoration considering master-slave distributed generators and topology reconfiguration. Appl Energy 2017;199:205–16.
[14] Billinton Roy. Reliability Evaluation of Power Systems. US: Springer; 1984.
[15] National Grid. STOR Market Info for TR24 – Appendix; 2015.
[16] Wang Y, Chen C, Wang J, Baldick R. Research on resilience of power systems under natural disasters—a review. IEEE Trans Power Syst. 2016;31:1604–13.
[17] Holling CS. Resilience and stability of ecological systems. Annu Rev Ecol Syst 1973;4:1–23.
[18] Berkeley AR, Wallace M. A framework for establishing critical infrastructure resilience goals: final report and recommendations by the council. Nat Infrastruct Advisory Council 2010.
[19] Chaudry M, Ekins P, Ramachandran K, Shakoor A, Skea J, Strbac G, et al. Building a

resilient UK energy system. Working paper Ref. UKERC/WP/ES/2009/023 UK Energy Research Centre, March 2009.
[20] Syrri AL, Martinez Cesena EA, Mancarella P. Contribution of microgirds to distribution network reliability. In: Proceedings of the 2015 IEEE Eindhoven PowerTech, Eindhoven, Netherlands, 28 June – 2 July 2015. p. 1–6.
[21] Wang Z, Wang J. Self-healing resilient distribution systems based on sectionalization into microgrids. IEEE Trans Power Syst 2015;30:3139–49.
[22] Chen C, Wang J, Qiu F, Zhao D. Resilient distribution system by microgrids formation after natural disasters. IEEE Trans Smart Grid 2016;7:958–66.
[23] Li Z, Shahidehpour M, Aminifar F, Alabdulwahab A, Al-Turki Y. Networked microgrids for enhancing the power system resilience. Proc IEEE 2017;105:1289–310.
[24] Chen C, Wang J, Ton D. Modernizing distribution system restoration to achieve grid resiliency against extreme weather events: an integrated solution. Proc IEEE 2017;105:1267–88.
[25] Aki H. Demand-side resiliency and electricity continuity: experiences and lessons learned in Japan. Proc IEEE 2017;105:1443–55.
[26] Jin M, Feng W, Marnay C, Spanos C. Microgrid to enable optimal distributed energy retail and end-user demand response. Appl Energy 2018;210:1321–35.
[27] Mousavizadeh S, Haghifam M, Shariatkhah M. A linear two-stage method for resiliency analysis in distribution systems considering renewable energy and demand response resources. Appl Energy 2018;211:443–60.
[28] Wang Z, Chen B, Wang J, Chen C. Networked microgrids for self-healing power systems. IEEE Trans Smart Grid 2016;7:310–9.
[29] Zheng M, Wang X, Meinrenken CJ, Ding Y. Economic and environmental benefits of coordinating dispatch among distributed electricity storage. Appl Energy 2018;210:842–55.
[30] Stadler M, Cardoso G, Mashayekh S, Forget T, DeForest N, Agarwal A, et al. Value streams in microgrids: a literature review. Appl Energy 2016;162:980–9.
[31] Haddadian H, Noroozian R. Multi-microgrids approach for design and operation of future distribution networks based on novel technical indices. Appl Energy 2017;185:650–63.
[32] Hatziargyriou N, Asano H, Iravani R, Marnay C. Microgrids. IEEE Power Energy Mag. 2007;5:78–94.
[33] Future Energy Scenarios: GB Gas and Electricity Transmission. Available online: http://fes.nationalgrid.com/media/1292/2016-fes.pdf (accessed on 29 October 2016).
[34] Zhang L, Zhou Y, Flynn D, Mutale J, Mancarella P. System-level operational and adequacy impact assessment of photovoltaic and distributed energy storage, with consideration of inertial constraints, dynamic reserve and interconnection flexibility. Energies 2017;10:989–1023.
[35] Met Office, UK, UK Climate Projections. Available: http://ukclimateprojections.metoffice.gov.uk/22563.
[36] Good N, Zhang L, Navarro-Espinosa A, Mancarella P. High resolution modelling of multi-energy domestic demand profiles. Appl Energy 2015;137:193–210.
[37] Duffie John A, Beckman William A. Solar Engineering of Thermal Processes (fourth ed.). John Wiley & Sons; 2013.
[38] Rahmani-Andebili M. Cooperative distributed energy scheduling in microgrids. Electric Distribution Network Management and Control. Springer, 2018. p. 235–54.
[39] Rahmani-andebili M, Shen H. Cooperative distributed energy scheduling for smart homes applying stochastic model predictive control. In: 2017 IEEE international conference on communications (ICC), Paris; 2017. p. 1–6.
[40] Martinez Cesena EA, Capuder T, Mancarella P. Flexible distributed multienergy generation system expansion planning under uncertainty. IEEE Trans Smart Grid 2016;7:348–57.
[41] Capuder T, Mancarella P. Techno-economic and environmental modelling and optimization of flexible distributed multi-generation options. Energy 2014;71:516–33.
[42] DECC and Parsons Brinckerhoff. Technical Assessment of the Operation of Coal and Gas Fired Plants. 2014. Available online: https://assets.publishing.service.gov.uk/government/uploads/system/uploads/attachment_data/file/387566/Technical_Assessment_of_the_Operation_of_Coal_and_Gas_Plant_PB_Power_FIN....pdf.
[43] Keith Bell. Methods and tools for planning the future power systems: issues and priorities. IET Special Interest Publication for the Council for Science and Technology on Modelling Requirements for the GB Power System Resilience during transition to Low Carbon Energy. Available online: https://www.theiet.org/sectors/energy/documents/modelling-5.cfm?type=pdf.
[44] Mai Trieu, Drury Easan, Eurek Kelly, Bodington Natalie, Lopez Anthony, Perry Andrew. Resource planning model: an integrated resource planning and dispatch tool for regional electric systems. Technical report NREL/TP-6A20-56723, 2013. Available online: https://www.nrel.gov/docs/fy13osti/56723.pdf.
[45] Amelin M. Comparison of capacity credit calculation methods for conventional power plants and wind power. IEEE Trans Power Syst 2009;24:685–91.
[46] Ancillary Services Report 2017 – Energy UK. Available online: https://www.energy-uk.org.uk/publication.html?task=file.download&id=6138 [accessed on 16 February 2018].
[47] Richardson I, Thomson M, Infield D, Clifford C. Domestic electricity use: a high-resolution energy demand model. Energy Build 2010;42:1878–87.
[48] Introduction to Triads. Available online: https://www.nationalgrid.com/sites/default/files/documents/44940-Triads%20Information.pdf [accessed on 5 January 2018].
[49] ETS. Solar Energy Calculator Sizing Guide n.d.: 31.
[50] Tesla. Powerwall; 2017.
[51] Future Energy Scenarios. UK Gas and Electricity Transmission; 2014. Available online: http://fes.nationalgrid.com/media/1298/2014-fes.pdf [accessed on 29 October 2016].
[52] Ofgem. Capacity Assessment Report 2013. Available online: https://www.ofgem.gov.uk/ofgem-publications/75232/electricity-capacity-assessment-report-2013.pdf.
[53] Zhou Y, Mancarella P, Mutale J. Generation adequacy in wind rich power systems: comparison of analytical and simulation approaches. In: Proceedings of the 2014 international conference probabilistic methods applied to power systems, Durham, UK, 7–10 July 2014. p. 1–6.